

# Drp1 widely, yet heterogeneously distributes in mice central nervous system

**Ting-Ting Luo**

Fourth Military Medical University

**Chun-Qiu Dai**

Lintong Rehabilitation and Convalescent Centre

**Jia-Qi Wang**

Fourth Military Medical University

**Zheng-Mei Wang**

Yan'an University

**Yi Yang**

Yan'an University

**Kun-Long Zhang**

Fourth Military Medical University

**Fei-Fei Wu**

Fourth Military Medical University

**Yan-Ling Yang**

Fourth Military Medical University

**Ya-Yun Wang** (✉ [wangyy@fmmu.edu.cn](mailto:wangyy@fmmu.edu.cn))

Fourth Military Medical University

---

## Research

**Keywords:** Mitochondria, Drp1, GABAergic neuron, glioma

**Posted Date:** March 25th, 2020

**DOI:** <https://doi.org/10.21203/rs.3.rs-18926/v1>

**License:**   This work is licensed under a Creative Commons Attribution 4.0 International License.

[Read Full License](#)

---

**Version of Record:** A version of this preprint was published at Molecular Brain on June 10th, 2020. See the published version at <https://doi.org/10.1186/s13041-020-00628-y>.

# Abstract

**Objectives:** Drp1 is widely expressed and plays a role in inducing mitochondrial fission process. It is confirmed that many diseases are associated with Drp1 and mitochondria. However, since the exact Drp1 is not specifically distributed, it is hard to determine the impact of anti-Drp1 molecules on human body and where the Drp1 inhibitor functions.

**Methods:** We visualized distribution of Drp1 in different brain regions, and explicated the relationship between Drp1 and mitochondria. GAD67-GFP knock-in mice were utilized to detect the expression patterns of Drp1 on the GABAergic neurons. And we further analyzed Drp1 expression in human malignant glioma tissue.

**Results:** Drp1 widely but heterogeneously distributed in central nervous system. Further observation indicated that Drp1 was highly and heterogeneously expressed in inhibitory neurons. Under transmission electron microscope, Drp1 distribution in dendrites was higher than other areas in neurons and only a small amount of Drp1 was located on mitochondria. In human malignant glioma, Drp1 fluorescence intensity increased from grade I-III, while grade IV showed the descending trend.

**Conclusion:** In this study, we observed Drp1 widely yet heterogeneously distributed in central nervous system. Drp1 heterogeneous distribution may be related with the occurrence and development of neurologic disease. We hope that the relationship between Drp1 and mitochondria may give the therapeutic guidance.

# Introduction

Dynamin-related protein (Drp1) is a ~ 80 kDa protein (monomer) which widely expresses in the brain, lung, heart, kidney, spleen, liver, hepatocystestestis and fibroblast of humans [1, 2]. Drp1 contains an N-terminal GTPase domain, a helical domain at the center and a GTPase effector domain (GED) at the C-terminus[3]. In cytoplasm, Drp1 exists in the shape of dimer or tetramer, and functions to induce mitochondrial fission process[4, 5]. Mitochondria are organelles that are responsible for several vital cell functions, including respiration, oxidative phosphorylation, and regulation of apoptosis[6]. Brain is one of the organs which need high energy. In brain, mitochondria move along cytoskeletal tracks to sites of high energy demand, like synapses, and change their morphology by fusion and fission in response to cellular metabolic activity[7]. Therefore, the balance of mitochondrial fission and fusion under the control of Drp1 is significant in maintaining brain function and energy supply[8]. Drp1 overexpression or mutation can disorder this balance. Mutant Drp1 causes mitochondria to collapse into perinuclear clusters which contain a highly interconnected network[4, 9]. Besides, lack of Drp1 results in mitochondrial elongation and connection of mitochondrial tubules[10]. These elongated mitochondria gradually accumulate oxidative damage and transform from elongated tubules into large spheres[11]. Such changes will finally leads into nervous system diseases.

It has been confirmed that many diseases are related with Drp1 and mitochondria, including neurodegenerative diseases and neuropathic pain[12]. Ju Gao et al revealed that mitochondrial dysfunction has been demonstrated as a common prominent early pathological feature in neurodegenerative diseases[13]. A large number of researches demonstrated that mitochondrial dysfunction is one of the best documented abnormalities and prominent early features in patients' brain of neurodegenerative diseases. Guo et al demonstrated that mitochondrial fission leads to the increase of ROS[14], and ROS increase will further induce neuropathic and inflammatory pain[15]. Ferrari et al found that in models of chemotherapy-induced neuropathic pain, ROS greatly induces Drp1-dependent mitochondrial fission[16]. To find the target treating strategy, some researchers identified some molecules as the Drp1 inhibitor including P110 and mdivi-1[16, 17].

However, the exact Drp1 distribution is unspecific, thus, the impact of the molecules on human body and in what range the Drp1 inhibitor takes the function is still unclear. So clarifying the specific Drp1 distribution in mitochondria and in neurons can be a good approach to the targeted treatment for the diseases.

In this study, we investigated the specific Drp1 distribution in neurons, GABAergic ( $\gamma$ -Aminobutyric acid) neuron and mitochondria under optical microscope and transmission electron microscope (TEM). Moreover, we also explored the expression changes of Drp1 in human malignant glioma from grade I-IV. Combining the results above, we conclude that Drp1 widely but heterogeneously distributes in central nervous system, and this heterogeneous distribution may be contribute to the neurologic diseases occurrence and development. As to the treatment, we also draw the conclusion that there are three possible targeted molecules. We hope that this research may give the novel insights towards disease targeted treatment in clinic.

## Results

### 1. Drp1 widely distributed in central nervous system

To explore the specific distribution of Drp1 in different brain regions, we observed the Drp1 expression in different brain regions and spinal cord.

#### 1.1 At protein level

In order to preliminarily explore whether the drp1 protein has regional specific distribution characteristics, western blot was used to detect the protein in cortex, hippocampus, cerebellum, thalamus, brain stem and spinal cord. The results showed that the Drp1 showed differences at protein level in six regions, with the highest expression in spinal cord and the lowest expression in cortex, hippocampus and cerebellum. (Fig. 1)

We next explored the exact Drp1 expression utilizing immunofluorescence staining. Drp1 expression was specified through the labeling intensity, which is classified as no signal (-), low signal (+), moderate signal

(++), high signal (+++), strong signal (++++), and “# ” presents strong non-specific labeling[18].

Results showed that Drp1 is highly expressed in layer 5 and 6a of the cerebral cortex, and in layer 2 some expression was also observed, but we didn't find the significant Drp1 expression in layer 1(Fig. 2). Drp1 was poorly expressed in hippocampus. However, some neurons in the layer of po and CA3sr expressed Drp1 in both soma and axon (Fig. 3). In cerebellum, Drp1 protein expression was mainly concentrated in Purkinje cell layer. Drp1 positive cells in pu layer were arranged in a single layer, separating the molecular layer (mo) and the granular cell layer (gr) (Fig. 4). In spinal cord, high Drp1 expression was observed in deep layer (VII, VIII, IX, X), which was slightly more than that in the superficial layer (I, II, III) (Fig. 5).

Among all the regions, we selected three nerve nuclei in which Drp1 was highly expressed (Fig. 6). In thalamus, Drp1 was highly expressed in LGd (dorsal part of the lateral geniculate complex), and LGv (ventral part of the lateral geniculate complex) (Fig. 6.A). In pons, Drp1 expression in PB (parabrachial nucleus), LC (locus ceruleus) and B (barrington's nucleus) was higher than that in other nuclei (Fig. 6.B). The labeling intensity in LGd, LGv, PB, DCO (Dorsal cochlear nucleus) and V (Facial motor nucleus) reached strong signal (+++). Details of the Drp1 protein expression in all regions are shown in Table.1. Moreover, based on the ALLEN Atlas, we also analyzed the proportion of different Drp1 labeling intensity in brain. The right part showed the Drp1 expression (Fig. 9.A). Results showed that low signal(+) accounts for the majority.

In conclusion, Drp1 is widely distributed in brain and spinal cord, which confirms the importance of Drp1 in CNS.

## **1.2 At mRNA level**

### **1.2.1 Probe titer determination**

Using the correctly sequenced recombinant plasmid as the template, the sequence containing the target gene fragment and SP6/T7 promoter joints at both ends were amplified. After amplification, we determined the probe concentration. Drp1 probe carrying SP6 and T7 was 281.27 ng/ul and 202.61 ng/ul, respectively.

### **1.2.2 Identification of probes and antisense probes**

Drp1 mRNA gene probes included the upstream and downstream promoter SP6 and T7 sequences, while the reverse sequence probes served as the negative control. The results showed the high hybridization signal of SP6 probe, and specific punctate granules were observed, while T7 probe showed no specific staining. Therefore, the positive sequence of the target gene Drp1 with SP6 as the promoter was selected for subsequent experiments.

### **1.2.3 Wide distribution of Drp1 mRNA in mice brain and spinal cord**

Results showed that Drp1 mRNA was widely distributed in all mice brain regions with strong hybridization signal and high specificity (Fig. 7).

In thalamus, Drp1 was highly expressed in LGd, LGv and IGL (intergeniculate leaflet of the lateral geniculate complex), with the fluorescence intensity of these three nucleuses reaching high signal (+++) (Fig. 7.G). In pons, the expression of Drp1 mRNA reached high signal (+++) in PB, LC and B. Expression in PCG (pontine central gray) was lower than that in these nucleuses (Fig. 7.L). In medulla, Drp1 mRNA was highly expressed in VCO (ventral cochlear nucleus) and DCO (dorsal cochlear nucleus) (Fig. 7.N). Drp1 mRNA was also widely distributed in the mice spinal cord with strong hybridization signal (Fig. 8).

Moreover, we compared the Drp1 labeling intensity at protein and mRNA level. Based on the ALLEN Atlas, the Drp1 signal was visualized in different brain slices. The left part showed the Drp1 mRNA expression. The right part showed the Drp1 protein expression. Results showed that Drp1 mRNA labeling intensity high signal (+++) accounted for the majority, and is higher than protein in both brain and spinal cord (Fig. 9).

In conclusion, Drp1 was widely distributed in the central nervous system but with heterogeneity, that some areas or nucleuses show the high Drp1 expression. The heterogeneity was also found between the Drp1 mRNA and protein level.

## **2. Mainly and highly expressed Drp1 in neurons**

The localization of Drp1 in the brain and spinal cord was consistent with what has been proposed in the traditional theory that Drp1 is widely distributed in CNS. However, unequivocal proof for the innervation is still lacking.

To specify the Drp1 distribution in neurons, we utilized double immunohistochemistry to label Drp1 and neurons with the anti-Drp1 antibody and anti-NeuN antibody. Among all results, three representative nucleuses were selected, and we found that the fluorescence of Drp1 (green) and NeuN (red) in the VPL (ventral posterolateral nucleus of the thalamus), ZI (zona incerta) and VII (facial motor nucleus) coincided well (Fig. 10).

In conclusion, Drp1 is mainly and highly expressed in neurons in the central nervous system, and in other parts of the nervous system besides neurons (such as glial cells), it could also be observed small amount of Drp1 expression.

## **3. Highly expressed Drp1 in GABAergic neurons**

GABAergic neurons are important inhibitory neurons, which is correlated with the development of many neurological diseases, including Huntington's disease, Alzheimer's disease, anxiety, panic disorder and epilepsy. To explore the effect of Drp1 on these diseases, we further clarified the distribution of Drp1 in GABAergic neurons. GAD67-GFP transgenic mice were used to observe the co-labeling of GAD67 and Drp1 in different brain regions.

We selected four Drp1 and GAD67 double staining nucleuses including MDRN (medullary reticular nucleus), PAS (parafascicular nucleus), cerebellum and VCO. Results indicated that Drp1 was overexpressed in cerebellum Purkinje cell layer, meanwhile, Drp1 and GAD67 in this area was also co-labeled well. Drp1 and GAD67 co-labeling was lower in the other nucleuses (Fig. 11).

## 4. Higher Drp1 distribution in dendrites and only a small amount of Drp1 located on mitochondria

As we discussed above, many neurologic diseases are confirmed the relationship with Drp1 and mitochondria[1]. Moreover, Drp1 is significant in maintaining mitochondrial function through the balanced control of mitochondrial fission and fusion[8]. Therefore, we observed the localization of mitochondrial Drp1 in brain nucleuses. Double labeling of Drp1 (green) and Mito-Red (red) in the LGd, SPIV (spinal vestibular nucleus) and IP (internal plexiform layer) showed that Drp1 and mitochondria coincided preferably. Both of Drp1 and Mito-Red were scattered around the nucleus. Mito-Red was concentrated on one side of the cell nucleus, while Drp1 expression showed no polarity and connected to form a network structure around the nucleus. Besides, the size of green (Drp1) granules was smaller than the red (Mito-Red) one, but the distribution range of Drp1 was wider than Mito-Red (Fig. 12). Considering that the fluorescent particles may overlap in vertical space, we utilized electron microscope for further observation.

We next investigated the distribution of mitochondrial Drp1 in PAG (periaqueductal gray) in the subcellular level through electron microscope. Moreover, we used statistical analysis to confirm the Drp1 distribution differences between dendrites, axons, axon terminals and somas.

Results showed that Drp1 was mainly expressed in cytoplasmic matrix, which was consistent with our results above. Dendrites could also find some expression, and a small amount of Drp1 was punctate distributed on mitochondrial membrane (Fig. 13.A).

Then, we made further investigation of the quantity of mitochondria and Drp1 in axons, axon terminals, dendrites and somas. 70 axons, 37 axon terminals, 36 dendrites and 6 somas were counted, and the average quantity of mitochondria and Drp1 in each part was calculated. Results showed that ratio of Drp1 to mitochondria in somas and in dendrites were significantly higher than the ratio in axons and in axon terminals.(Fig. 13)

We further analyzed Drp1 expression proportion under TEM. We utilized Kruskal-Wallis test to analyze Drp1 expression differences. Kruskal-Wallis test results showed that  $H = 39.854$ ,  $P < 0.001$ , according to the test standard of  $\alpha = 0.05$ , rejecting  $H_0$ , it can be considered that Drp1 expression was different in axons, axon terminals, dendrites and somas. Drp1 expression in dendrites was higher than in axons (adjusted  $P < 0.001$ ), and Drp1 expression in dendrites was higher than in axon terminals (adjusted  $P < 0.001$ ). There was no difference in Drp1 expression between axons and axon terminals, axons and

somas, axon terminals and somas, or between dendrites and somas (adjusted  $P > 0.05$ ).  
(Table 2&Fig. 13.D)

## 5. Drp1 expression in human malignant glioma tissue reached the highest value in grade III and then descended

Alongside neurons, we also analyzed Drp1 expression in human malignant glioma tissue. With the normal human brain tissue as control tissue, grade I showed the juvenile gliomas tissue. Grade II-IV showed the mild, moderate and severe malignancy gliomas tissue, respectively. Ten highest Drp1 fluorescence intensity points were selected in every grade, and mean value of fluorescence intensity of each grade was calculated (Table 3&Fig. 14)

Results showed that, from grade I-III, the mean value of Drp1 fluorescence intensity showed an increasing trend. In grade IV, mean value of Drp1 fluorescence intensity significantly reduced.(Fig. 14.C)

## Discussion

1.  
Drp1 widely but heterogeneously distributes in central nervous system.

This study reveals that Drp1 is widely distributed in central nervous system at both protein and mRNA level, which firmly demonstrates the importance of Drp1. Moreover, Drp1 is widely expressed in the cytoplasm but scarcely distributed on mitochondria, which only accounts for about 5%. This result is consistent with previous studies[19, 20]. However, Drp1 distribution also shows the heterogeneity.

1.1  
The expression of Drp1 in different kinds of neurons is heterogeneous.

In inhibitory neurons, we found high Drp1 expression. Figure 4 showed that Drp1 was highly expressed in the dendrites of the Mo layer (the dendrites of the Purkinje cell layer) in the cerebellar cortex. The neuron in this layer is the important inhibitory neuron[21]. In addition, Drp1 is also expressed in the second layer of the cerebral cortex, which is the external granular layer[22]. Drp1 expression difference in cerebral cortex may be related to the diverse cell types of each layer. The second layer contains a large number of granular cells, the majority of which are GABAergic inhibiting neurons[23].

1.2  
Drp1 expression in neurons also shows heterogeneity.

All immunofluorescence results showed that Drp1 was highly expressed and distributed around the nucleus, and IEM results showed that Drp1 was mainly expressed in dendrites. In addition, we found that Drp1-positive protuberant structures (long strips in Fig. 4), may possibly be the axons or dendrites. Therefore, it can be speculated that the distribution of Drp1 is mainly concentrated in the dendrites.

As the vital factor in regulating mitochondrial fission process, Drp1 should be expressed in all cells. However, as is shown in Fig. 9, Drp1 protein and mRNA expression is different in same region, and no Drp1 expression was found in some neurons, which might suggest that some other molecules could also induce mitochondrial fission process. Further investigation is still needed.

2.

Drp1 heterogeneous distribution may contribute to the occurrence and development of neurological diseases.

As we discussed above, mitochondrial dysfunction is involved in the occurrence and development of neurologic disease[24]. Drp1 mutation promotes mitochondrial dysfunction[25]. A large number of researches also demonstrated that GABA is related with the development of neurological diseases.

GABA is the major inhibitory neurotransmitter in CNS. It is confirmed that dysfunction of GABA metabolism or GABAergic neurons is associated with many neurological diseases, including Huntington's disease, Alzheimer's disease, anxiety, panic disorder and epilepsy[26, 27]. However, whether Drp1 directly affects these diseases through GABAergic neuron is still unclear.

Therefore, we analyzed the Drp1 expression in GABAergic neurons. The results of this study showed that Drp1 distribution is mainly concentrated in the initial part of GABAergic neurons, dendrites, axons and neuron mitochondria. This heterogeneous Drp1 distribution may contribute to neurological diseases occurrence and development.

As we discussed in introduction, some molecules targeted to Drp1 have been found. However, the impact of the molecules mentioned above on human body and in what diseases these molecules can be used in clinic still need to be further studied. Therefore, heterogeneous Drp1 distribution in GABAergic neurons may give us the targeted treating guidance toward the GABA related diseases.

3.

Drp1 expression in human malignant glioma further demonstrates Drp1's significance in cells.

Based on the results above, we make the conclusion that Drp1 widely but heterogeneously distributes in central nervous system, which firmly indicates the importance of Drp1. However, in central nervous system, the connection between glial cells and neurons also plays the vital role in regulating normal brain function. In Fig. 10, alongside neurons, we found that in other parts of the nervous system such as glial cells, small amount of Drp1 expression could also be observed.

Therefore, we further analyzed Drp1 expression in human malignant glioma tissue. Compared the mean value of Drp1 fluorescence intensity in every grade, we found the increasing Drp1 fluorescence intensity trend from grade I-III. In grade IV, mean value of Drp1 fluorescence intensity significantly reduced. The highest fluorescence intensity in moderate malignancy indicated that the mitochondrial dynamic changes reach the maximum. In grade IV, normal tissue was destroyed, so fluorescence intensity significantly reduced. Such expression changes were also found in other malignant tumors[28, 29]. Thus, results of

Drp1 expression in human malignant glioma further demonstrate Drp1's significance in cells, and may give us the guidance that Drp1 changes could function as the early indicator of malignant diseases.

4.

Inhibiting Drp1 may be the novel target for neurological diseases treatment.

When mitochondrion is going to divide, Drp1 will translocate from cytoplasm to mitochondrial outer membrane with the help of receptors and adapters[30], and assemble into ring-like structures on mitochondrial outer membrane, leading into mitochondrial fission[31, 32]. When Drp1 translocates abnormally to the mitochondrial membrane, mitochondrial dynamic homeostasis regulated by Drp1 will be broken, leading to mitochondrial morphological changes[17]. Therefore, inhibiting the Drp1 harboring in neurons may be the novel target in treating the neurological diseases[33].

For treatment, we identify three molecules which can inhibit Drp1. P110 can effectively inhibit the translocation of Drp1 from cytoplasm to mitochondria, and inhibit the binding of Drp1 to Fis1, thus inhibiting mitochondrial division[17]. Hirotsugu Kanda et al found the significant increase of Drp1 in neuropathic pain model. Further study demonstrated that intrathecal Drp1 antisense oligodeoxynucleotide (ODN) could decrease the spinal Drp1 expression[34]. Besides ODN, mdivi-1 is another Drp1 inhibitor. Luiz F also revealed that mdivi-1 could attenuate the neuron pathologic changes[16].

Nowadays, there is still no better method for the prevention of neurological diseases like the AD, HD. And the disease diagnosis often lags behind the disease development. Therefore, new target drugs need to be developed urgently. It is clear that P110, mdivi-1[35, 36] and OND can effectively inhibit Drp1 translocation from cytoplasm to mitochondria. However, the impact of the molecules mentioned above on human body and whether it can be efficiently and conveniently applied in clinic still need to be further studied.

This study also needs improvements in several parts. It is much better to use Drp1 knockout mice in the investigation of Drp1 distribution, but these Drp1 knockout mice can't survive. Moreover, the phosphorylation status of Drp1 is essential for its interaction with Mff, and takes the vital role in regulating mitochondrial dynamic, but this study didn't observe the phosphorylation Drp1 status. We will investigate it in the following research.

In this study, we observed the Drp1 distribution in brain and found that Drp1 widely yet heterogeneously distributes in central nervous system. Drp1 heterogeneous distribution may be involved in the occurrence and development of neurological diseases. Moreover, we identified three targeted molecules for treatment. We hope that this research on the relationship between Drp1 and mitochondria in neurons may be helpful in the molecular therapy, and give the clinical guidance for neurological diseases treatment. As the vital factor for mitochondrial dynamics, future studies are still needed on the Drp1 distribution and translocation beyond the pathological changes.

# Materials And Methods

## 1. Animals

Adult male C57BL/6 mice and GAD67-GFP knock-in mice (Center of Lab Animals, Fourth Military Medical University, Xi'an, China), weighed 25–30 g. The generation and characterization of the GAD67-GFP knock-in mice has been described in our previous research [37].

Experimental mice were housed and treated in strict accordance with the Rules for Animal Care[38]and Use for Research and Education of Fourth Military Medical University.

## 2. Experimental procedure

### 2.1 Intrathecal Mito-Red loading

In order to explore the exact Drp1 distribution on mitochondria, intrathecal Mito-Red loading was utilized to visualize mitochondrial morphology.

The characterization of MitoTracker® has been described in our previous research [15]. Mito-Red (MitoTracker® Deep Red FM, Invitrogen, USA) was injected intrathecally. Mito-Red was qualified to concentration of 100 nM dissolving in 1:1 mixture of dimethylsulfoxide(DMSO), and saline and 5 µl solution were injected into subarchnoid space from a small hole on L3 vertebral lamina using a Hamilton syringe attached to 10-gauge needle. Control groups were injected with 5 µl DMSO using the same methods.

After 4 days, mice were perfused with 0.01 M phosphate-buffered saline (PBS; pH 7.4) and 4% formaldehyde in PBS successively after anesthesia. Brains were removed into 30% sucrose solution for tissue dehydration. After dehydration, brains were sliced into 30µm using freezing microtome (CM1950, Leica). Incubation of Drp1 and fluorescence developing were same as immunofluorescence staining.

### 2.2 Immunofluorescence staining

In order to map the Drp1 protein expression in central nervous system, immunofluorescence staining was utilized in three kinds of animals, including normal adult C57BL / 6 mice, intrathecal injection of Mito-Red mice and GAD67- GFP mice. Light should be avoided during Mito-Red mice operation, other operations were same to C57BL / 6 mice and GAD67- GFP mice. Anti-Drp1 antibody incubation for its spontaneous fluorescence was performed only in Mito-Red mice and GAD67- GFP mice.

Mice were perfused with 0.01 M PBS and 4% formaldehyde in PBS successively after anesthesia. Brains were removed into 30% sucrose solution for tissue dehydration. After dehydration, brains were sliced into 30µm using freezing microtome (CM1950, Leica, Germany)). To determine the distribution and localization of Drp1, slices were transferred to PBS and then 10% calf serum for 30 min. Then slices were incubated with 1:250 diluted anti-Drp1 antibody (ab184247, Abcam, UK) at 4 °C overnight. In order to avoid false positive results, Tempol (ROS scavenger) was utilized to treat the tissue. After anti-

drp1 antibody incubation, the tissue was treated in Tempol (380 nmol / 5  $\mu$  L) solution for 1 h. Then slices were incubated with 1:500 diluted secondary antibody (goat anti-rabbit IgG; Sigma, St. Louis, MO, USA) for 2 h. Slides were rinsed triple times for 15 min with 0.01M PBS after incubation. No signal was detected when the primary or secondary antibody was omitted. Images were recorded using confocal microscopy (FV1000, Olympus, Japan) connected to an inverted microscope. Figures were checked with brain atlas (Paxinos and Watson, 1998) and Allen brain Atlas (2003) and prepared using Adobe Photoshop 7.0.

## 2.3 Fluorescence in situ hybridization (FISH)

In order to observe the Drp1 mRNA distribution in central nervous system, fluorescence in situ hybridization was utilized. Drp1 gene primer was designed and used in our previous research[39].

Drp1 gene upstream primer 5'-3': GCTCAGTGCTGGAAAGCCTA; downstream primer 5'-3': GATGGATTGGCTCAGGGCTT, amplification length: 297 bp.

Construction of probe plasmids: cDNA of C57BL/6 mice were amplified by PCR with primers; gel was used to recycle the PCR products; the products were linked to carriers at room temperature with T7 and SP6 promoters at both ends (Roche, Switzerland); the plasmids were transformed into E.coli DH5alpha and cultured; the probe plasmids were extracted by Plasmid Extraction Kit (Tiangen, China) and then were sequenced.

Probe preparation: using the sequenced plasmid as template, PCR amplification was carried out with T7 and SP6 specific primers, PCR products were recycled by Omega Gel Recycle Kit (Omega, USA), probe was transcribed into cRNA in vitro by T7-RNA polymerase/ SP6-RNA polymerase.

Mice were anaesthetized with 25% uratan solution (6 ml/kg, intraperitoneal injection), rinsed the blood from right atrial appendage with 30 ml (0.01 M DEPC-PBS), then rinsed the blood with 4% paraformaldehyde 100 ml. After perfusion, the mice brain and lumbar spinal cord (lumbar enlargement) were removed completely, and were put in 4% paraformaldehyde fixative solution in the refrigerator at 4°C for 24 hours. Coronal sections were cut by Leica CM1950 (Germany). Brain slices and spinal cord slices were 30 and 25 $\mu$ m thick, respectively. Slices were treated in 0.1 M DEPC-PB containing 2% H<sub>2</sub>O<sub>2</sub> for 10 minutes, 0.1 M DEPC-PB containing 0.3% Triton X-100 for 20 minutes and acetylation solution for 10 min at room temperature, respectively. Slices were incubated in hybridization buffer at 58°C for 1 h. Drp1 cRNA probe was added to the above-mentioned hybridization buffer (final concentration: 1  $\mu$ g/ml) and incubated in the hybridization oven at 58°C for 20–24 hours. Rinsed slices and treated it with RNA enzyme solution for 5 minutes at room temperature, 2 \* SSC and 0.2 x SSC (diluted by 20 \* SSC, with 2% NLS) was used to rinse the slices twice, 20 minutes each time, 37°C, respectively. Slices were incubated with antibody POD-anti-DIG (1:1500) for whole night,  $\beta$ -D-Glucose (1:100) for 30 minutes, FITC-avidin (1:500), for 3 hours and DAPI (1:1000) for 15 minutes at room temperature. After incubation, the slices were observed and photographed by laser confocal microscopy (FV1000, Olympus, Japan)

## 2.4 Western blotting and analysis

In order to preliminarily explore whether the drp1 protein has regional specific distribution characteristics, western blot was used to detect the protein in mice central nervous system.

10% SDS–polyacrylamide gel electrophoresis (SDS-PAGE) was prepared [40]. Equal amounts of protein (30 µg) were electrophoresed on 10% SDS–polyacrylamide gels and transferred 2 h onto PVDF-membrane, which were incubated with anti-Drp1 antibody (1:1500, Abcam, UK) and secondary antibody (horse-radish peroxidase-conjugated anti-rabbit IgG from donkey, Amersham, Biosciences, Piscataway, NJ, USA)[40]. Immunoblots were developed using ECL kit (K-12045-D10; Advansta, USA) and BIO-RAD ChemiDoc MP lighting machine, results were quantified by computerized scanning densitometry and analyzed by Image J software.

## 2.5 Immunoelectron microscopy (IEM)

In order to explore Drp1 localization on mitochondria in subcellular level, we utilized immunoelectron microscopy for further observation.

The shooting area was PAG. After perfusion, the brain was removed immediately and was cut into small pieces (PAG area). The tissue was fixed with 4% paraformaldehyde fixative of 15% saturated picric acid, and then was sliced into 50 µm thick. And slices were treated into frozen section by liquid nitrogen, and were incubated with 20% donkey serum (diluted by 0.05 M TBS) for 30 minutes, rabbit anti-Drp1 antibody (1:100, Abcam, UK), 2% donkey blood were added afterwards for 24 hours' incubation. After primary incubation, sheep anti-rabbit (1:100, Nanoprobes, USA) labeled with immune gold particles (NG) and 2% donkey serum (0.05 M TBS diluted) were added for further incubation overnight at room temperature. Silver-enhanced reaction: HQ Silver Kit (Nanoprobes, USA) treatment for 7–14 minutes, then dripped into Ainitator, B moherntor, C activator reagent one drop, respectively. After 7 minutes reaction, the slices were poured into distilled water to stop the reaction and observed under optical microscope (AH-3, Olympus, Japan). After observation, slices were incubated with 1% starvation acid solution and 0.2 M PB for 35 minutes in 1:1 dilution, then treated with 70%~100% gradient alcohol and propylene oxide for dehydration. Slices were polymerized in the embedding agent overnight. After stained with lead citrate, slices could be observed and photographed under electron microscope (JEM1400, Tokyo, Japan).

The criteria for distinguishing different parts are as follows: 1. Soma: Soma contains less heterochromatin, the color is light, and the nucleolus is large and obvious. The cytoplasm contains rough endoplasmic reticulum, free ribosome, Golgi complex, neurofilament and microtubule; 2. Mitochondrion: Mitochondrion is the organelle surrounded by two layers of membrane, which is oval or long strip, and its length changes greatly. 3. Dendrite: Dendrites contain Nissl body, mitochondria, Golgi complex, smooth endoplasmic reticulum, neurofilament and microtubule. Clusters of ribosomes often appear with irregular outline, prominent ratchet like accessory structures including hypertrophic mitochondria, microtubules, and post prominent specialized structures. 4. Axons: The axon structure is thin, smooth and without spines. Axons are usually separated from the cell body. Under the electron microscope, the main cell components in axons are free ribosome, mitochondria, neurofilament and microtubule. With the extension of axons, rough endoplasmic reticulum and ribosome gradually decreased or even disappeared. Some

axons are surrounded by myelin sheath. 5. Axon terminals: The axon terminals are spherical, expanded and thickened to form presynaptic membrane. Synaptic vesicles and several mitochondria could be found in axon terminal.

## **2.6 Glioma tissues screening and staining**

### **2.6.1 Glioma tissues screening**

Patient glioma tissues were provided by Xijing hospital. All patients provided written informed consent before glioma tissues recruitment. After screening, 3 cases of hairy cell astrocytoma, 6 cases of diffuse astrocytoma, 6 cases of anaplastic astrocytoma, 13 cases of glioblastoma, 13 cases of oligodendrocytoma, 13 cases of anaplastic oligodendrocytoma and 6 cases of paracancerous tissue were included in this study.

### **2.6.2 HE staining**

HE staining was conducted according to routine protocols. 4- $\mu$ m sections were obtained from each paraffin block utilizing pathological microtome (Leica RM2235, Germany). After deparaffinization and rehydration, sections were stained with hematoxylin solution (Solarbio, G1080, China) for 5 min, stained with eosin (Solarbio, G1100-100, China) for 3 min and re-immersed in alcohol and xylene. The mounted slides were then examined and photographed using inverted microscope (Nikon CI-S, Japan) and imaging system (Nikon DS-U3, Japan).

### **2.6.3 Glioma staining**

The slides of glioma cells were taken out from PBS and rinsed in PBS for 3 times at room temperature, 10 min/time; 10% calf serum was used for 2 hours incubation; slides were incubated in anti-rabbit-anti-drp1 (Abcam, ab184247, 1:1000, UK) overnight in a wet and dark box at room temperature; rinsed slices in PBS at room temperature for 3 times, 10 min / time in next day; incubated the slices in anti-a488-anti-rabbit (Abbkine, 1:500, USA) for 2 hours; rinsed slices 3 times in PBS at room temperature, 10 min / time; sealed slices with fluorescent sealing agent and photographed under confocal microscope (FV1000, Olympus, Japan).

## **3. Statistical analysis**

Data are presented as the mean  $\pm$  standard error of the mean (SEM). One-way repeated-measures ANOVA was used for the analysis of differences between the experimental groups. Kruskal-Wallis test was used to confirm the Drp1 distribution differences between dendrites, axons, axon terminals and somas under IEM.  $P < 0.05$  was considered statistically significant.

## **Abbreviations**

Drp1: dynamin-related protein; GED: GTPase effector domain; GABA:  $\gamma$ -Aminobutyric acid; FISH: fluorescence in situ hybridization; IEM: immunoelectron microscopy; TEM: transmission electron

microscope; LGd: dorsal part of the lateral geniculate complex; LGv: ventral part of the lateral geniculate complex; PB: parabrachial nucleus; LC: locus ceruleus; B: barrington's nucleus; DCO: Dorsal cochlear nucleus; Ⅹ: Facial motor nucleus; IGL: intergeniculate leaflet of the lateral geniculate complex; PCG: pontine central gray; VCO: ventral cochlear nucleus; VPL: ventral posterolateral nucleus of the thalamus; ZI: zona incerta; MDRN: medullary reticular nucleus; PAS: parafascicular nucleus; SPIV: spinal vestibular nucleus; IP: internal plexiform layer; PAG: periaqueductal gray; ODN: oligodeoxynucleotide

## **Declarations**

## **Ethics approval and consent to participate**

Patient glioma tissues were provided by Xijing hospital, The Fourth Military Medical University. The scientific use of the human material was conducted in accordance with the Declaration of Helsinki. All patients provided written informed consent before glioma tissues recruitment. All procedures were approved and performed in accordance with the Rules for Animal Care and Ethical Guidelines for Research and Education of Fourth Military Medical University.

## **Consent for publication**

Not Applicable.

## **Availability of data and materials**

The datasets used and analyzed during the current study are available from the corresponding author on reasonable request.

## **Competing interests**

The authors have declared that no conflict of interest exists.

## **Funding**

This work was supported by grants from the National Natural Science Foundation of China (81870415, 81470843) and Shaanxi Key R&D Program (2018JZ8003-2018KA01, 2018ZDXM-SF-082)

## **Author contributions**

Yayun Wang and Yanling Yang designed this manuscript. Chunqiu Dai and Zhengmei Wang wrote the report. Tingting Luo and Yi Yang conducted the experiment. Jiaqi Wang, Kunlong Zhang and Feifei Wu

participated in figures drawing.

## Acknowledgments

We thank to patients and their families, clinical staff for technical assistance, patient care, sampling and tissue data acquisition. We also thank to Xijing hospital for providing glioma tissue samples for this study.

## References

1. Oliver, D. and P.H. Reddy, *Dynamics of Dynamin-Related Protein 1 in Alzheimer's Disease and Other Neurodegenerative Diseases*. Cells, 2019. **8**(9).
2. Reddy, P.H., et al., *Dynamin-related protein 1 and mitochondrial fragmentation in neurodegenerative diseases*. Brain Res Rev, 2011. **67**(1-2): p. 103-18.
3. Ford, M.G., S. Jenni, and J. Nunnari, *The crystal structure of dynamin*. Nature, 2011. **477**(7366): p. 561-6.
4. Smirnova, E., et al., *Dynamin-related protein Drp1 is required for mitochondrial division in mammalian cells*. Mol Biol Cell, 2001. **12**(8): p. 2245-56.
5. Wu, W., et al., *OPA1 overexpression ameliorates mitochondrial cristae remodeling, mitochondrial dysfunction, and neuronal apoptosis in prion diseases*. Cell Death Dis, 2019. **10**(10): p. 710.
6. Gusdon, A.M., et al., *Exercise increases mitochondrial complex I activity and DRP1 expression in the brains of aged mice*. Exp Gerontol, 2017. **90**: p. 1-13.
7. Saxton, W.M. and P.J. Hollenbeck, *The axonal transport of mitochondria*. J Cell Sci, 2012. **125**(Pt 9): p. 2095-104.
8. Otera, H., N. Ishihara, and K. Mihara, *New insights into the function and regulation of mitochondrial fission*. Biochim Biophys Acta, 2013. **1833**(5): p. 1256-68.
9. Wanders, R.J. and H.R. Waterham, *Biochemistry of mammalian peroxisomes revisited*. Annu Rev Biochem, 2006. **75**: p. 295-332.
10. Ren, X., et al., *Resveratrol Ameliorates Mitochondrial Elongation via Drp1/Parkin/PINK1 Signaling in Senescent-Like Cardiomyocytes*. Oxid Med Cell Longev, 2017. **2017**: p. 4175353.
11. Cho, B., et al., *Physiological and pathological significance of dynamin-related protein 1 (drp1)-dependent mitochondrial fission in the nervous system*. Exp Neurobiol, 2013. **22**(3): p. 149-57.
12. Qi, Z., et al., *Dynamin-related protein 1: A critical protein in the pathogenesis of neural system dysfunctions and neurodegenerative diseases*. J Cell Physiol, 2019. **234**(7): p. 10032-10046.
13. Gao, J., et al., *Abnormalities of Mitochondrial Dynamics in Neurodegenerative Diseases*. Antioxidants (Basel), 2017. **6**(2).
14. Gibellini, L., et al., *Natural Compounds Modulating Mitochondrial Functions*. Evid Based Complement Alternat Med, 2015. **2015**: p. 527209.

15. Guo, B.L., et al., *Significant changes in mitochondrial distribution in different pain models of mice*. Mitochondrion, 2013. **13**(4): p. 292-7.
16. Ferrari, L.F., et al., *Role of Drp1, a key mitochondrial fission protein, in neuropathic pain*. J Neurosci, 2011. **31**(31): p. 11404-10.
17. Dai, C.Q., et al., *p53 and mitochondrial dysfunction: novel insight of neurodegenerative diseases*. J Bioenerg Biomembr, 2016. **48**(4): p. 337-47.
18. D'Agata, V., et al., *Distribution of parkin in the adult rat brain*. Prog Neuropsychopharmacol Biol Psychiatry, 2002. **26**(3): p. 519-27.
19. MacDonald, J.A., et al., *A nanoscale, multi-parametric flow cytometry-based platform to study mitochondrial heterogeneity and mitochondrial DNA dynamics*. Commun Biol, 2019. **2**: p. 258.
20. Woods, D.C., *Mitochondrial Heterogeneity: Evaluating Mitochondrial Subpopulation Dynamics in Stem Cells*. Stem Cells Int, 2017. **2017**: p. 7068567.
21. Fecher, C., et al., *Cell-type-specific profiling of brain mitochondria reveals functional and molecular diversity*. Nat Neurosci, 2019. **22**(10): p. 1731-1742.
22. Molina, V., et al., *Cell cycle analysis in the rat external granular layer evaluated by several bromodeoxyuridine immunoperoxidase staining protocols*. Histochem Cell Biol, 2017. **148**(5): p. 477-488.
23. Stumm, R.K., et al., *Neuronal types expressing mu- and delta-opioid receptor mRNA in the rat hippocampal formation*. J Comp Neurol, 2004. **469**(1): p. 107-18.
24. Lim, T.K., et al., *Mitochondrial and bioenergetic dysfunction in trauma-induced painful peripheral neuropathy*. Mol Pain, 2015. **11**: p. 58.
25. Joshi, A.U., et al., *Drp1/Fis1 interaction mediates mitochondrial dysfunction, bioenergetic failure and cognitive decline in Alzheimer's disease*. Oncotarget, 2018. **9**(5): p. 6128-6143.
26. Wong, C.G., T. Bottiglieri, and O.C. Snead, 3rd, *GABA, gamma-hydroxybutyric acid, and neurological disease*. Ann Neurol, 2003. **54 Suppl 6**: p. S3-12.
27. Solas, M., E. Puerta, and M.J. Ramirez, *Treatment Options in Alzheimer s Disease: The GABA Story*. Curr Pharm Des, 2015. **21**(34): p. 4960-71.
28. Ma, J.T., et al., *Effects of Dynamin-related Protein 1 Regulated Mitochondrial Dynamic Changes on Invasion and Metastasis of Lung Cancer Cells*. J Cancer, 2019. **10**(17): p. 4045-4053.
29. Aggarwal, S., et al., *Depletion of dAKAP1-protein kinase A signaling islands from the outer mitochondrial membrane alters breast cancer cell metabolism and motility*. J Biol Chem, 2019. **294**(9): p. 3152-3168.
30. Tagaya, M. and K. Arasaki, *Regulation of Mitochondrial Dynamics and Autophagy by the Mitochondria-Associated Membrane*. Adv Exp Med Biol, 2017. **997**: p. 33-47.
31. Santel, A. and S. Frank, *Shaping mitochondria: The complex posttranslational regulation of the mitochondrial fission protein DRP1*. IUBMB Life, 2008. **60**(7): p. 448-55.

32. Chang, C.R. and C. Blackstone, *Drp1 phosphorylation and mitochondrial regulation*. EMBO Rep, 2007. **8**(12): p. 1088-9; author reply 1089-90.
33. Song, Y., et al., *Inhibition of Drp1 after traumatic brain injury provides brain protection and improves behavioral performance in rats*. Chem Biol Interact, 2019. **304**: p. 173-185.
34. Kanda, H., et al., *Inhibition of Mitochondrial Fission Protein Reduced Mechanical Allodynia and Suppressed Spinal Mitochondrial Superoxide Induced by Perineural Human Immunodeficiency Virus gp120 in Rats*. Anesth Analg, 2016. **122**(1): p. 264-72.
35. Zhou, K., et al., *RIP1-RIP3-DRP1 pathway regulates NLRP3 inflammasome activation following subarachnoid hemorrhage*. Exp Neurol, 2017. **295**: p. 116-124.
36. Wu, Q., et al., *Mitochondrial division inhibitor 1 (Mdivi-1) offers neuroprotection through diminishing cell death and improving functional outcome in a mouse model of traumatic brain injury*. Brain Res, 2016. **1630**: p. 134-43.
37. Wang, Y.Y., et al., *Expression patterns of 5-HT receptor subtypes 1A and 2A on GABAergic neurons within the spinal dorsal horn of GAD67-GFP knock-in mice*. J Chem Neuroanat, 2009. **38**(1): p. 75-81.
38. Zimmermann, M., *Ethical guidelines for investigations of experimental pain in conscious animals*. Pain, 1983. **16**(2): p. 109-10.
39. Luo, T.T., et al., *Distribution of mitochondrial dynamin-related protein 1 mRNAs in amygdala complex of mice based on the FISH technique*. Chinese Journal of Neuroanatomy, 2017. **33**(2): p. 149-154.
40. Yang, Y.L., et al., *Abnormal chloride homeostasis in the substantia nigra pars reticulata contributes to locomotor deficiency in a model of acute liver injury*. PLoS One, 2013. **8**(5): p. e65194.

## Tables

### **Table.1 Drp1 protein and mRNA expression in different brain regions and spinal cord**

Drp1 expression was specified through the labeling intensity, which were classified as low signal(+), moderate signal(++), high signal(+++),strong signal(++++) . "N/A" represents this region was not observed.

Regions		Intensity		
		Protein	mRNA	
<b>Cerebral cortex</b>	BLA, Basolateral amygdalar nucleus	++	+++	
	DGN/Apo, Dentate gyrus, polymorph layer	++	+++	
	mPFC, medial prefrontal cortex	+	++	
<b>Cerebral nuclei</b>	LS, Lateral septal nucleus	+++	+++	
	MS, Medial septal nucleus	+++	+++	
	MEA, Medial amygdalar nucleus	+	+++	
	CEA, Central amygdalar nucleus	+	+++	
	PAL, Pallidum	++++	N/A	
<b>Thalamus</b>	LGd, Dorsal part of the lateral geniculate complex	+++	+++	
	LGv, Ventral part of the lateral geniculate complex	+++	+++	
	VPL, Ventral posterolateral nucleus of the thalamus	+	+++	
	IGL, Intergeniculate leaflet of the lateral geniculate complex	++	+++	
	RT, Reticular nucleus of the thalamus	+++	+++	
	AD, Anterodorsal thalamic nucleus	+++	N/A	
	VAL, Ventral anterior N/A lateral complex of the thalamus	+++	N/A	
<b>Hypothalamus</b>	VMH, Ventromedial hypothalamic nucleus	+++	N/A	
	ZI, Zonaincerta	N/A	+++	
<b>Midbrain</b>	PAG, Periaqueductal gray	++	+++	
	SNr, Substantia nigra, reticular part	+++	+++	
	DR, Dorsal nucleus raphe	+++	++++	
	VTA, Ventral tegmental area	+++	N/A	
	IPN, Interpeduncular nucleus	+	N/A	
<b>Pons</b>	PB, Parabrachial nucleus	++++	++++	
	LC, Locus ceruleus	+++	++++	
	B, Barrington's nucleus	+++	++++	
	POR, Superior olivary complex, periolivary region	++++	++++	
<b>Medulla</b>	CN, Cochlear Nuclei	++++	++++	
	VII, Facial motor nucleus	++++	+++	
	SPVC, Spinal trigeminal nucleus, caudal	+++	N/A	
	NTS, Nucleus of solitary tract	++	N/A	
	CU, Cuneate nucleus	+++	N/A	
	MDRN, Medullary reticular nucleus	+++	N/A	
	SPIV, Spinal vestibular nucleus	++	N/A	
	PAS, Parasolitary nucleus	+	N/A	
	<b>Cerebellum</b>			
	<b>Spinal Cord</b>	SIMpu, Simple lobule, Purkinje layer	++++	++++
Lamina I		+	++++	
Lamina II		+	+++	

Lamina III	+	+++
Lamina IV	+	+++
Lamina V	+	+++
Lamina VI	+	+++
Lamina VII	++	+++
Lamina VIII	++	+++
Lamina IX	++	+++
Lamina X	++	+++

---

**Table.2 Kruskal-Wallis test results of Drp1 expression in different brain areas.**

Kruskal-Wallis test results showed that  $H = 39.854$ ,  $P < 0.001$ , according to the test standard of  $\alpha = 0.05$ , rejecting  $H_0$ , it can be considered that Drp1 expression was different in axon, axon terminal, dendrite and soma.

Group	N	Median	Quartiles	H	P
axon	70	.008	.009	39.854	.000
axon terminal	37	.009	.013		
dendrite	36	.025	.038		
soma	6	.022	.019		

**Table.3 Value of Drp1 fluorescence intensity in different tumor grades**

Ten highest Drp1 fluorescence intensity points were selected in every grade, and mean value of fluorescence intensity of each grade was calculated.

	Control	grade I	grade II	grade III	grade IV
<b>1</b>	0.49	0.027	0.273	0.123	0.254
<b>2</b>	0.433	0.134	0.362	0.326	0.273
<b>3</b>	0.538	0.232	0.267	0.618	0.364
<b>4</b>	0.54	0.647	0.539	1.167	0.508
<b>5</b>	0.45	0.454	0.789	0.9	0.67
<b>6</b>	0.269	0.314	0.773	0.556	0.247
<b>7</b>	0.513	0.18	0.245	0.585	0.332
<b>8</b>	0.148	0.19	0.195	0.252	0.218
<b>9</b>	0.335	0.173	0.381	0.657	0.339
<b>10</b>	0.6	0.234	0.402	1.139	0.316
<b>Mean value</b>	0.4316	0.2585	0.4226	0.6323	0.3521

## Figures

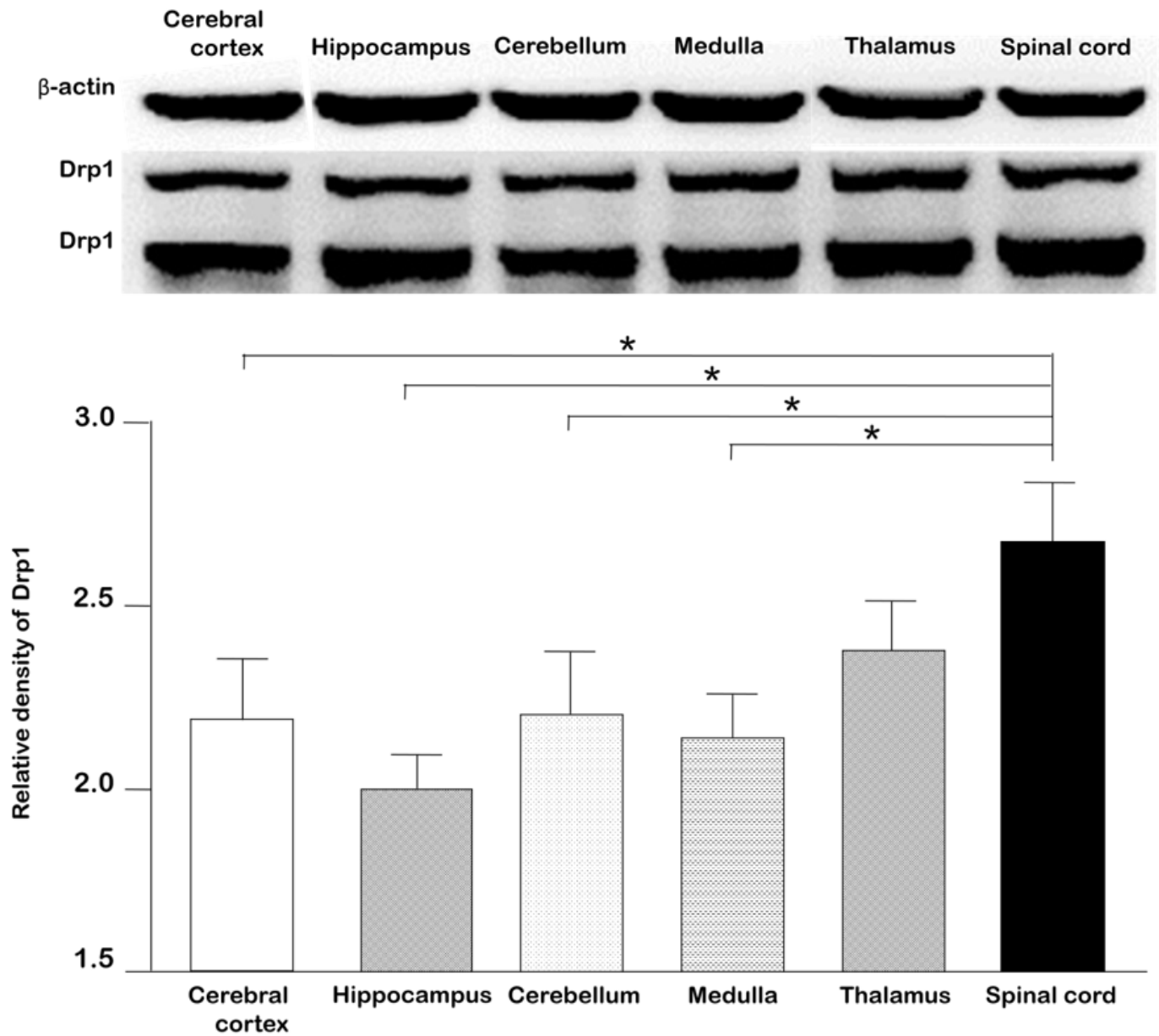


**Figure 1**

Drp1 protein content in brain and spinal cord. Western blot results in cortex, hippocampus, cerebellum, thalamus, brain stem and spinal cord. Drp1 protein level in six regions showed differences. The highest expression was in spinal cord and the lowest expression was in cortex, hippocampus and cerebellum.

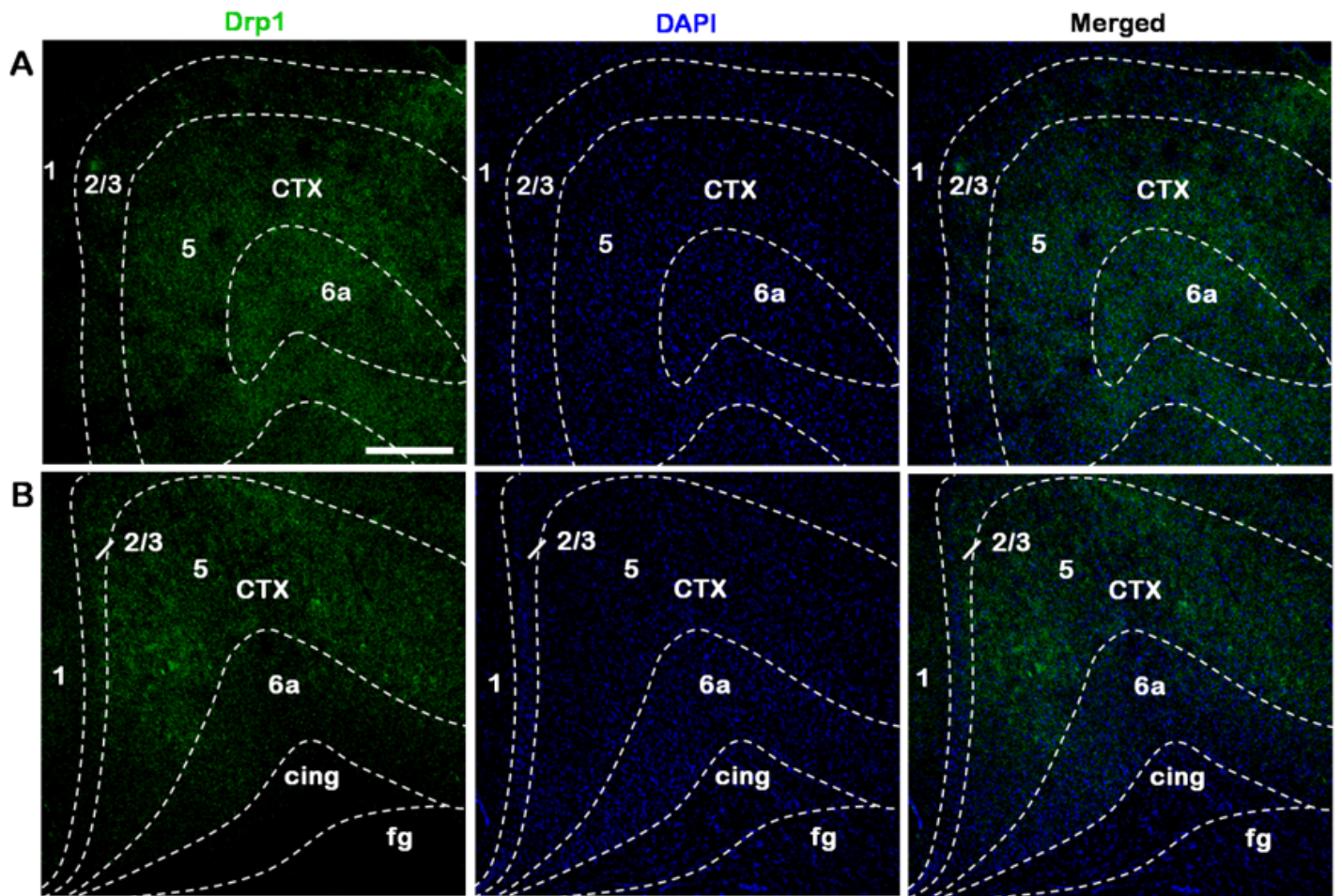


**Figure 2**

Drp1 distribution in Cerebral cortex. A and B are two different sections of CTX. Drp1 almost not expressed in the first layer of CTX, and specific staining results appeared in the second/third layer. Compared with other layers, Drp1 expression in the fifth layer was more than others. Bar = 200  $\mu\text{m}$  A, B

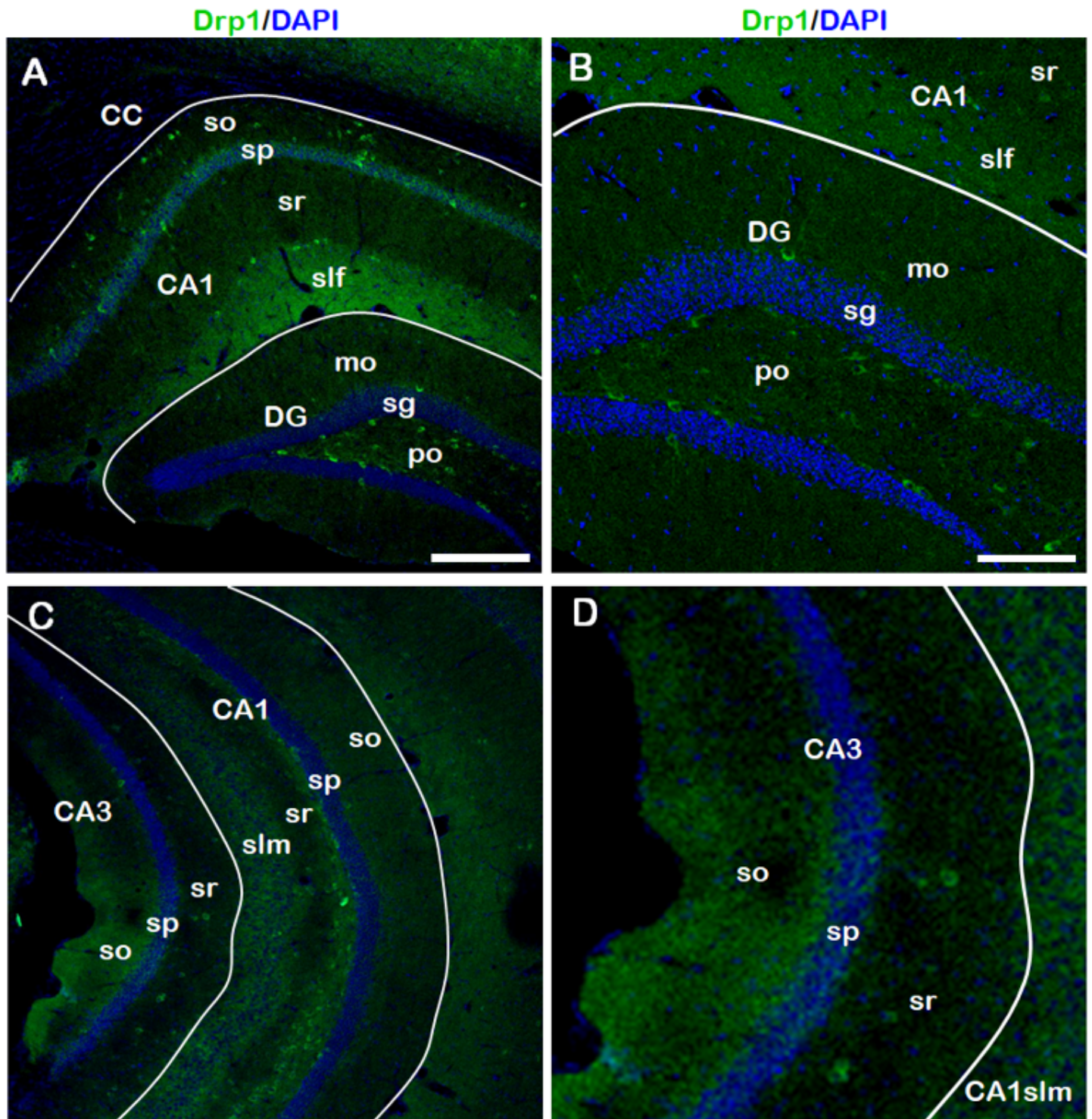


**Figure 3**

Drp1 (green) and DAPI (blue)'s distribution in CA1 and DG regions. Drp1 was low expressed in CA1, DG-mo (molecule layer of dentate gyrus) and DG-sg (granular cell layer of dentate gyrus). Drp1 in DG-po (polymorphic layer of dentate gyrus) as found high expressed. B was the magnified image of A. From B, we could see that some Drp1-positive cells in DG-mo and DG-po regions had protuberance around them (white arrows), possibly be the axons. C. Drp1 distribution in CA3. D was the magnified image of C. D

showed the protuberance in individual Drp1-positive cells in CA3sr region. Bar = 200  $\mu$ m (A, C), 100  $\mu$ m (B, D)

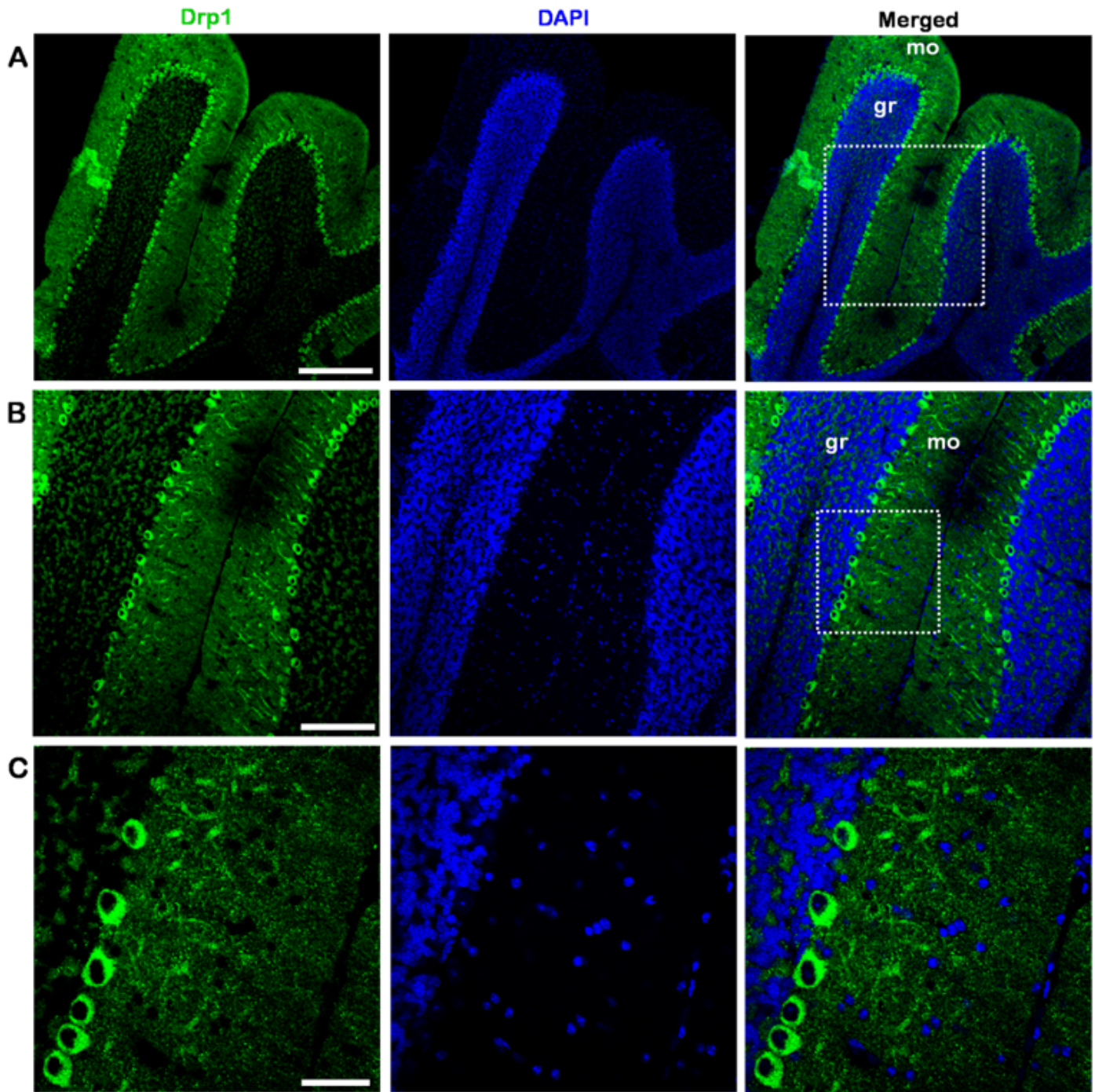


**Figure 4**

Drp1 distribution in Cerebellum A. Drp1 expression in cerebellar cortex. Drp1 expressed in pu layer. B was the magnified image of A. C was the magnified image of B. Drp1 was expressed in the cytoplasm around the nucleus (DAPI). In addition, Drp1-positive protuberant structures were also found in Mo region, which were long strips, possibly be the axons. Bar = 200  $\mu$ m (A); 100  $\mu$ m (B); 30  $\mu$ m (C)

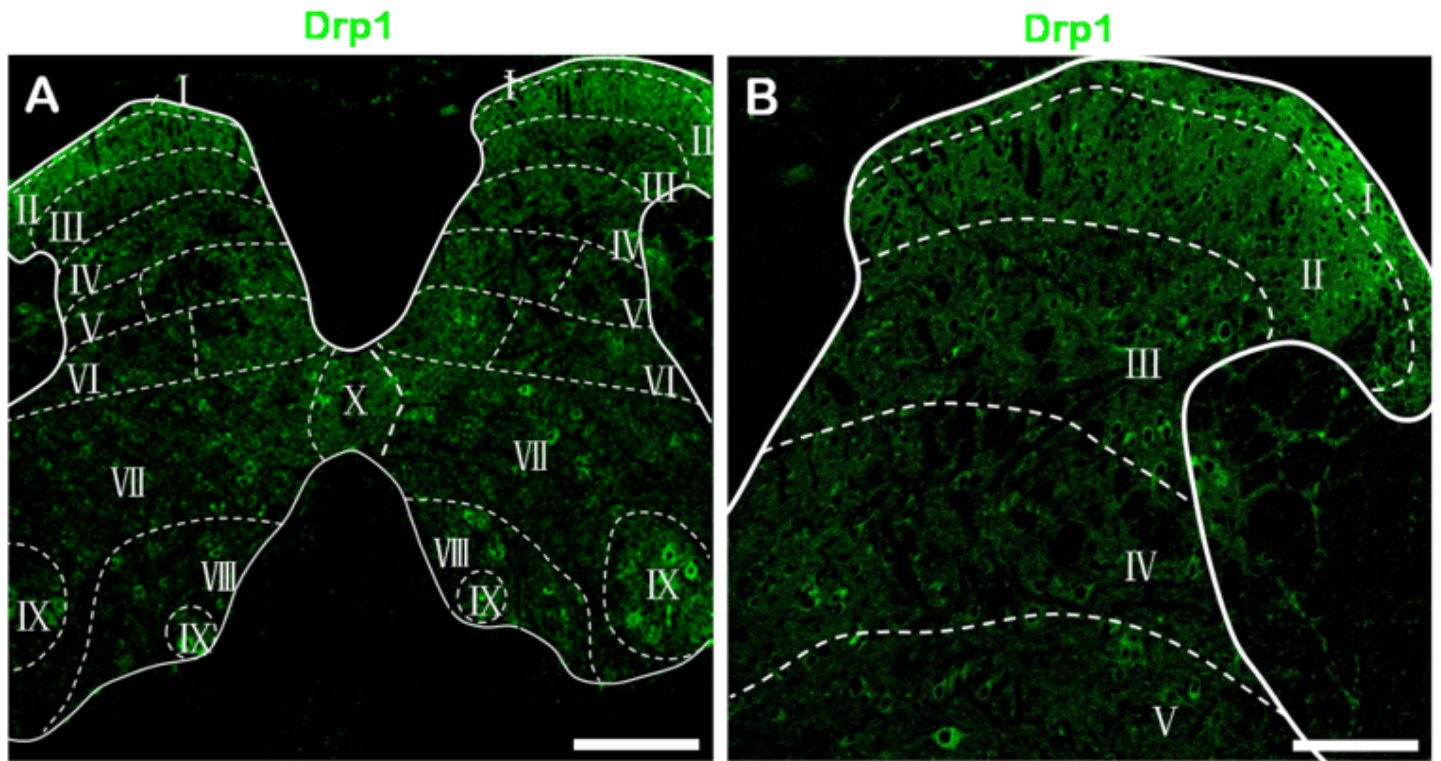


**Figure 5**

Drp1 distribution in Spinal Cord A. Full view of the spinal cord. In deep layer (VII, VIII, IX, X), Drp1 expression is slightly more than that in the superficial layer (I, II, III). B, In spinal dorsal horn, Drp1 was low expressed. Bar = 200  $\mu\text{m}$  (A); 100  $\mu\text{m}$  (B)

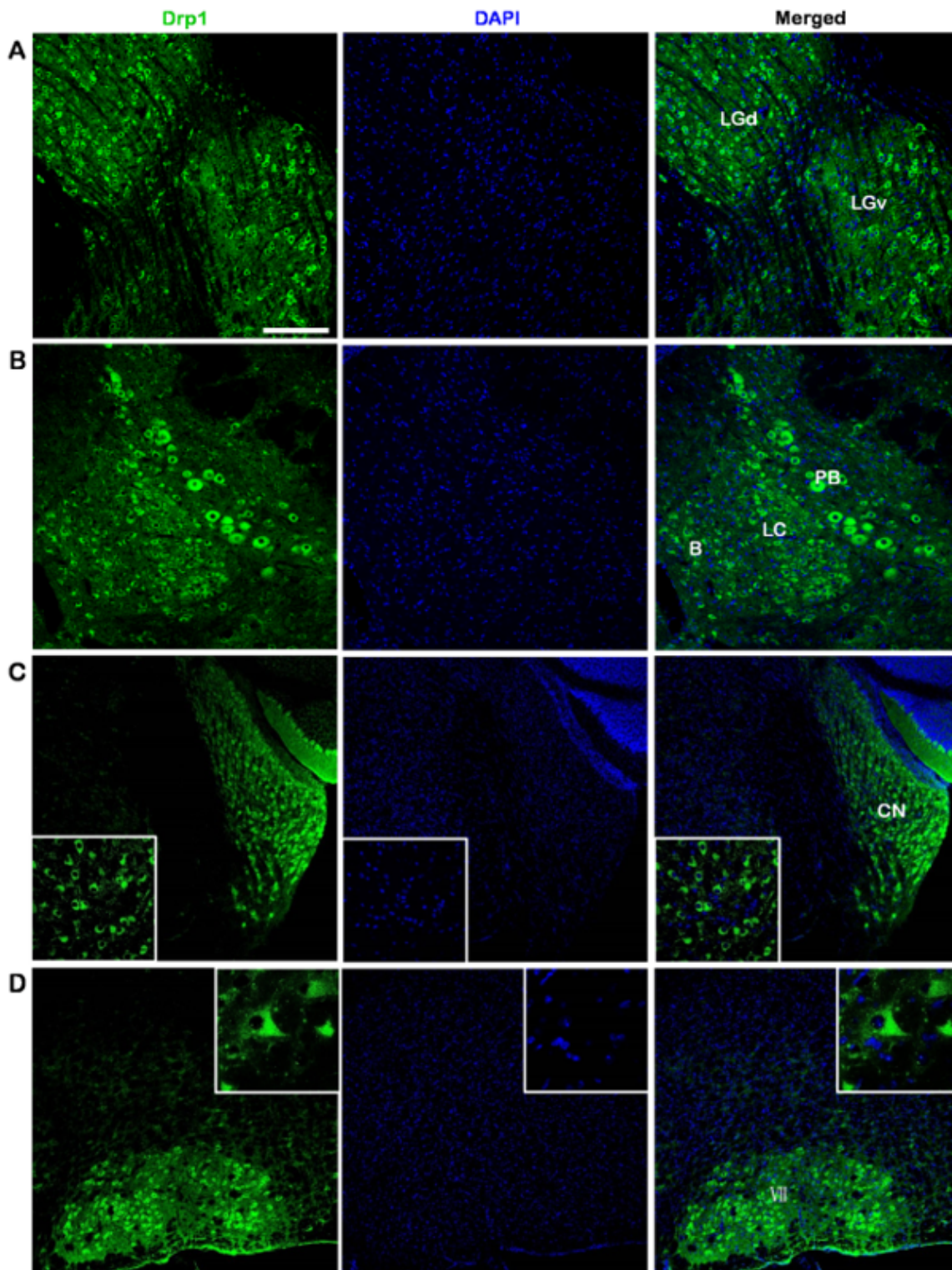


**Figure 6**

Brain regions with high Drp1 expression Drp1 was highly expressed in LGd and LGv (A), parabrachial nucleus (PB) (B), cochlear nucleus (CN) (C) and facial motor nucleus (VII) (D). Bar = 100  $\mu$ m (A-D)

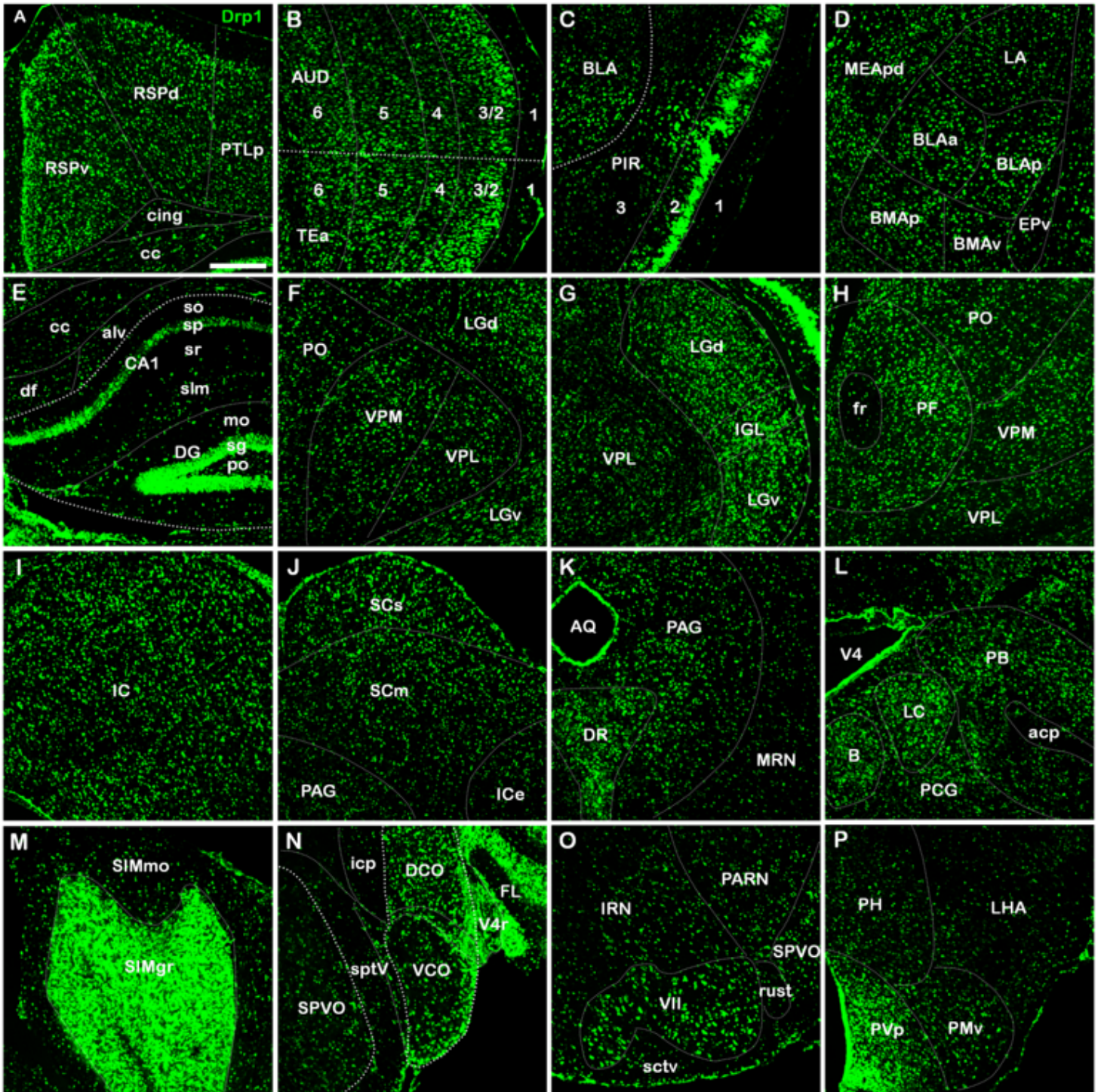


**Figure 7**

Drp1 mRNA distribution in whole brain Drp1 mRNA was highly expressed in the nuclei shown in A-P. Bar = 200  $\mu$ m (A - P)

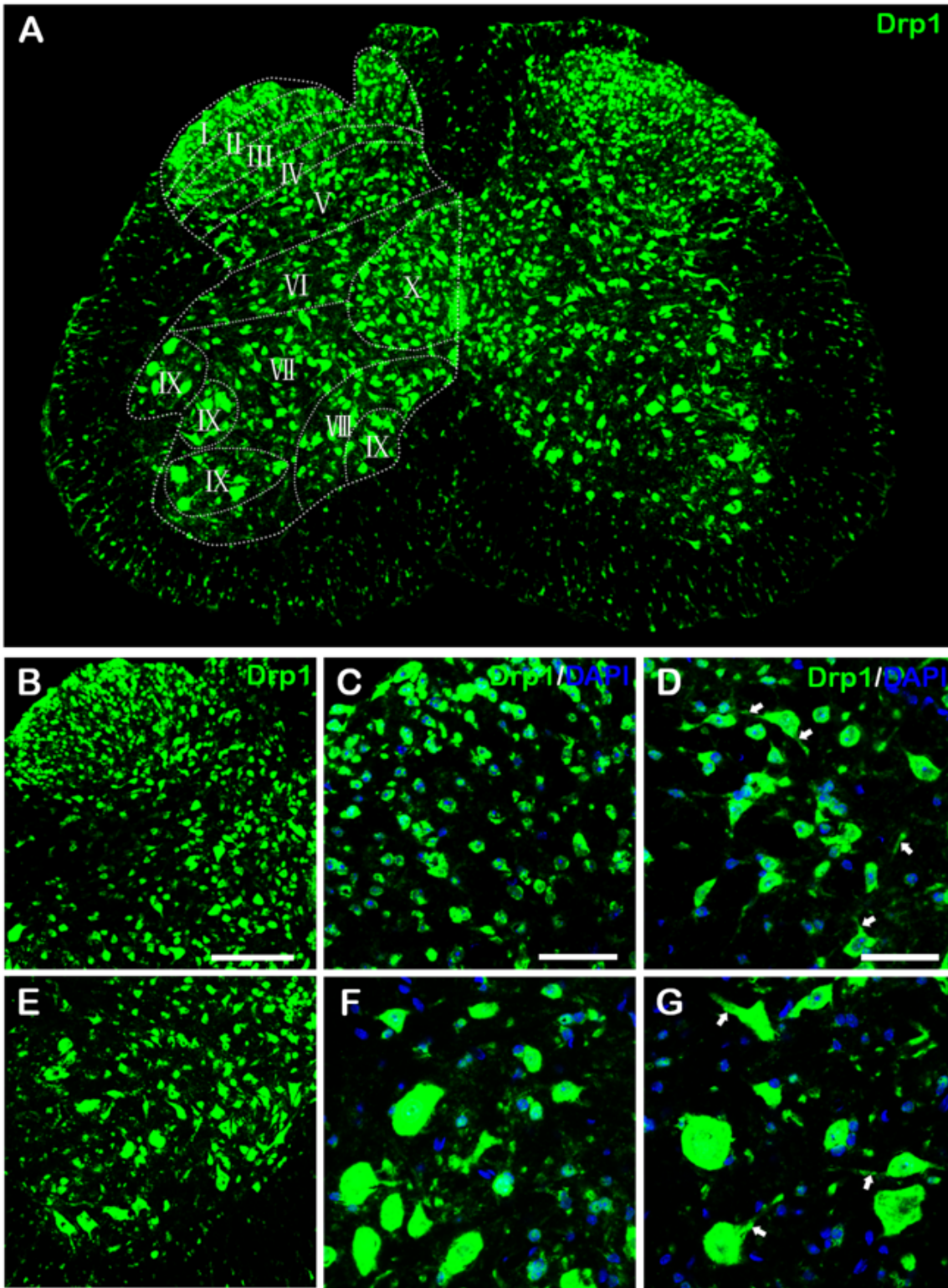


**Figure 8**

Drp1 mRNA expression in spinal cord A, full view of the spinal cord, Drp1 mRNA are highly expressed in layer I. The cells in IX are larger, and axon-like structures can be seen. B, enlargement of the spinal dorsal horn, C/D were the magnified image of B, D showed the cells in layer IV and V, in which the protuberant structure (white arrow) can be seen. C, enlargement of the spinal anterior horn, F and G are the cells of the

IX layer. The protuberances around the cell body can be seen (white arrow). Bar = 100  $\mu\text{m}$  (B, E); 30  $\mu\text{m}$  (C, D, F, G)

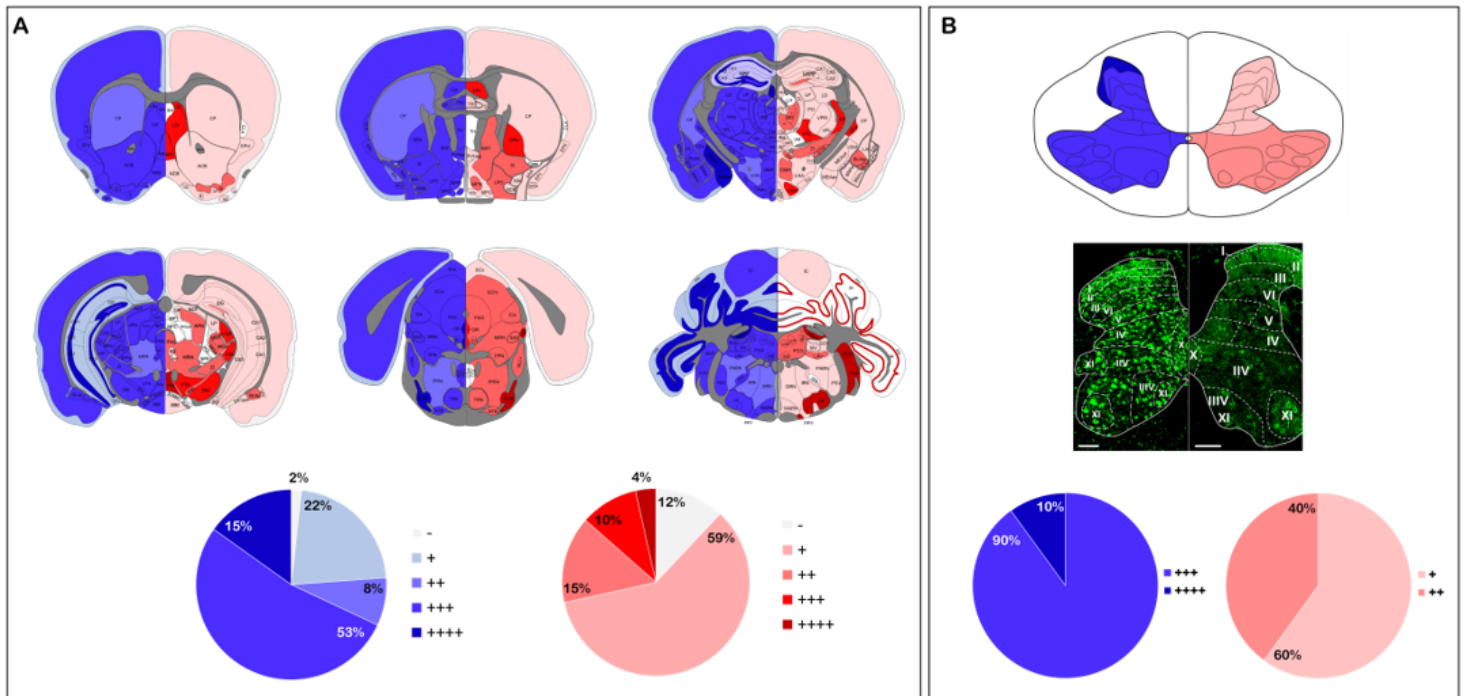


**Figure 9**

Comparison of Drp1 mRNA and protein expressions A. Comparison of Drp1 mRNA and protein expressions in brain. Based on the ALLEN Atlas, the Drp1 signal was visualized in different brain slices. The left part shows the Drp1 mRNA expression. Drp1 mRNA data analysis reveals that low signal (+) accounts for the majority; The right part shows the Drp1 protein expression. Drp1 labeling intensity, high signal (+++)accounts for the majority. B. Comparison of Drp1 mRNA and protein expression in spinal cord. Drp1 mRNA was highly expressed in layer I. The cells in IX are larger, and axon-like structures can be seen; In deep layer (VII, VIII, IX, X), Drp1 protein expression is slightly more than that in the superficial layer (I, II, III). Bar = 200  $\mu\text{m}$

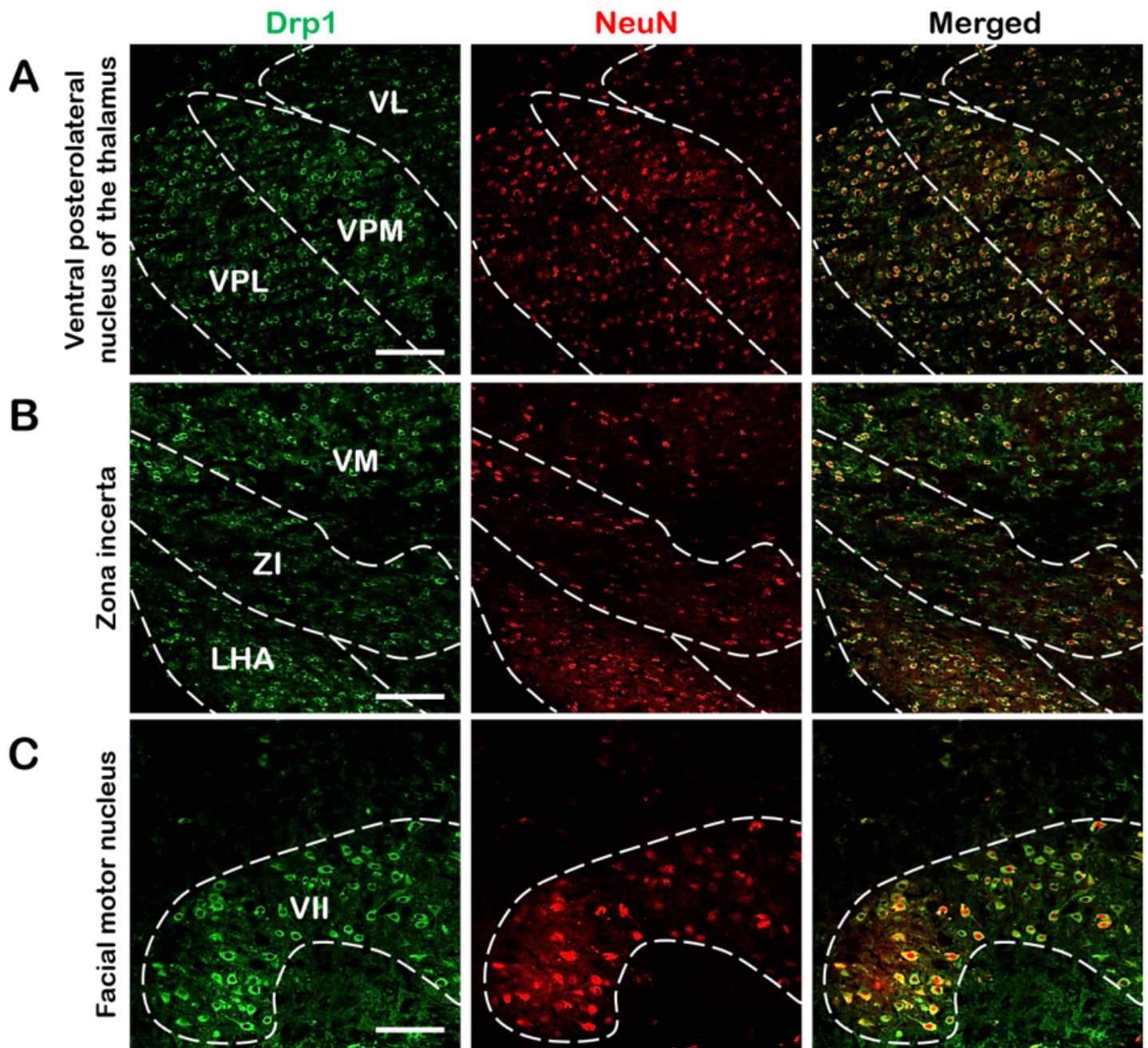
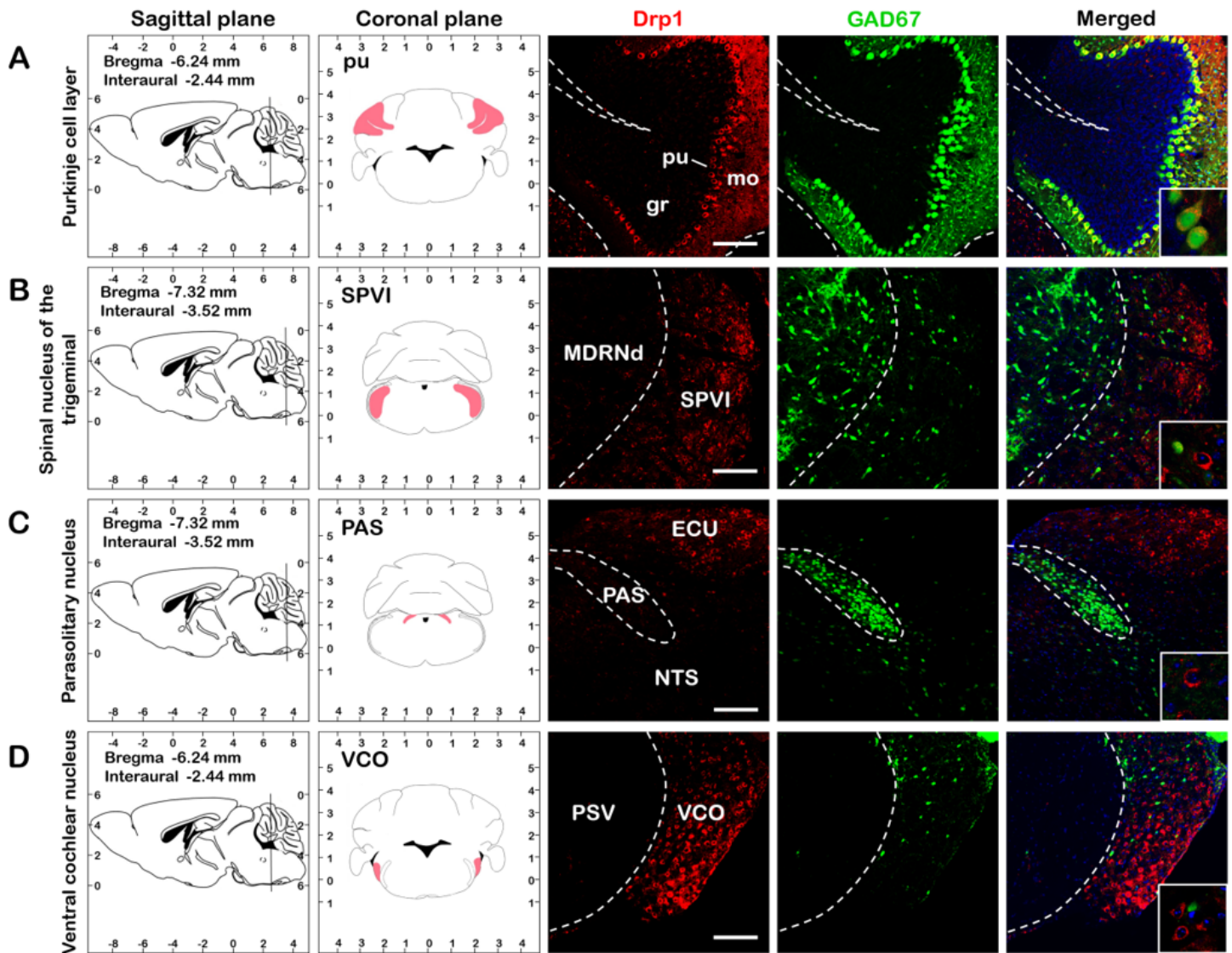


Figure 10

Co-labeling of Drp1 and NeuN A. Drp1 and NeuN staining results in VPL B. Drp1 and NeuN staining results in ZI C. Drp1 and NeuN staining results in VII It can be seen that in these nuclei, Drp1 and NeuN were completely co-labeled. Bar = 100  $\mu$ m



**Figure 11**

Results of double staining of Drp1 and GAD67 A.Drp1 and GAD67 were double stained in cerebellum. The pu cells expressed Drp1 and also expressed GAD67, which was completely co-labeled. B.Drp1 and GAD67 in medulla. Drp1 was highly expressed in SPVI, and was slightly expressed in MDRNd, while GAD67 was lower in SPVI, higher in MDRNd. C.Drp1 and GAD67 in PAS. Results showed that Drp1 and GAD67 were not co-labeled in most of this area. D. Drp1 and GAD67 in medulla. Drp1 is highly expressed in VCO, GAD67 is only expressed in several cells in VCO. Bar = 100  $\mu$ m

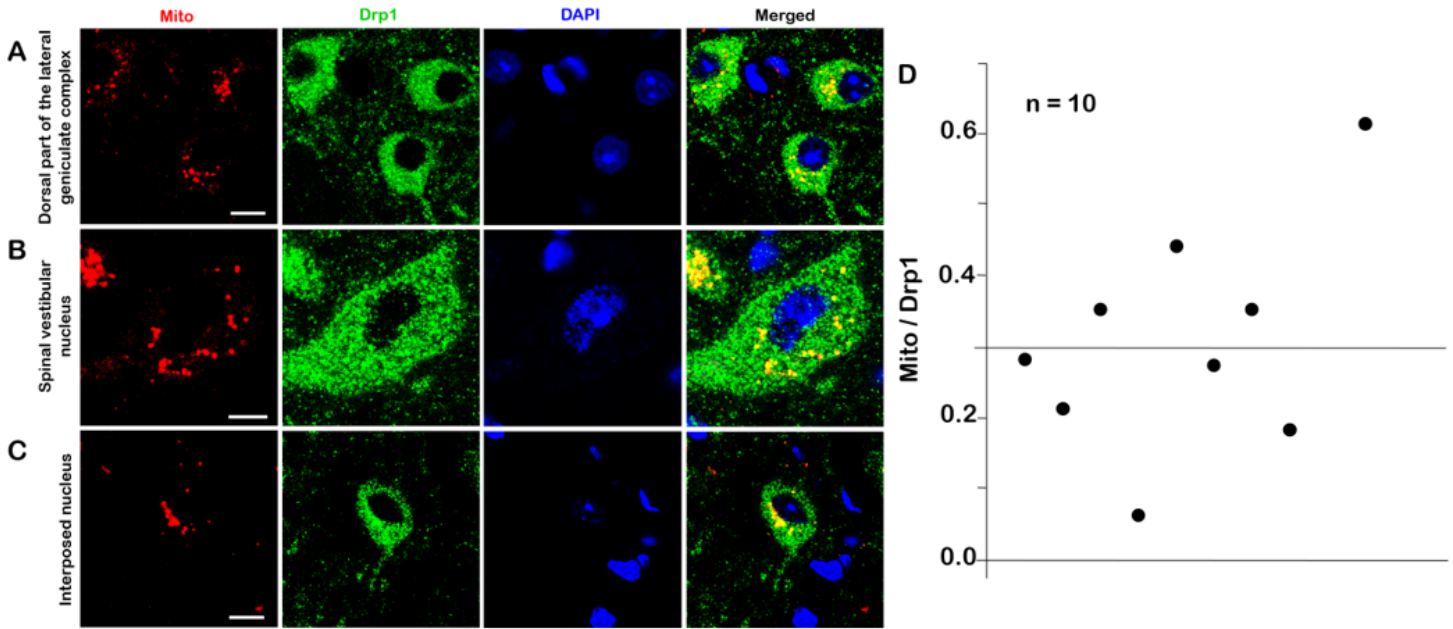


**Figure 12**

Distribution of Drp1 and Mito-Red in brain nucleus A. Drp1, Mito-Red and DAPI in dorsal part of the LGd. Drp1 and Mito were scattered around the nucleus. B. Drp1, Mito and DAPI in SPIV. C. Drp1, Mito and DAPI in the IP. D. Ratio of Mito / Drp1 fluorescence area. 10 neurons were selected for further analysis. Results showed that the ratio fluctuated around 0.3. Bar = 10 $\mu$ m

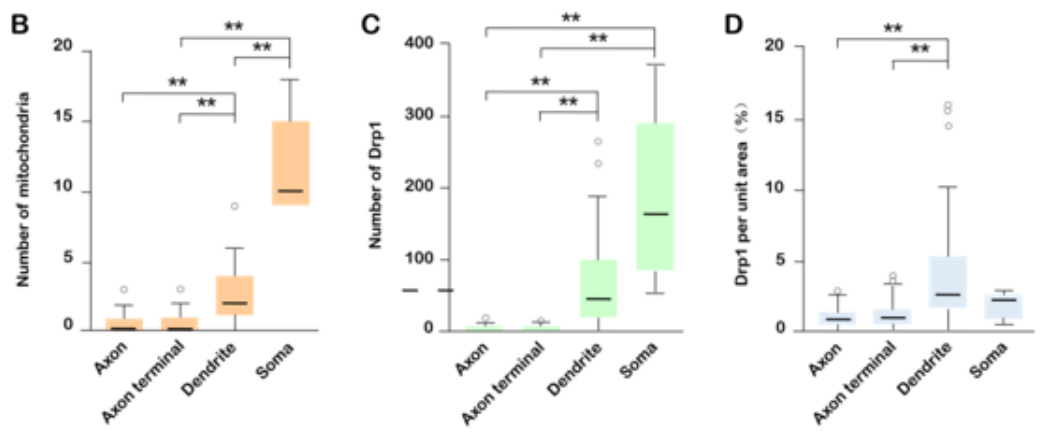
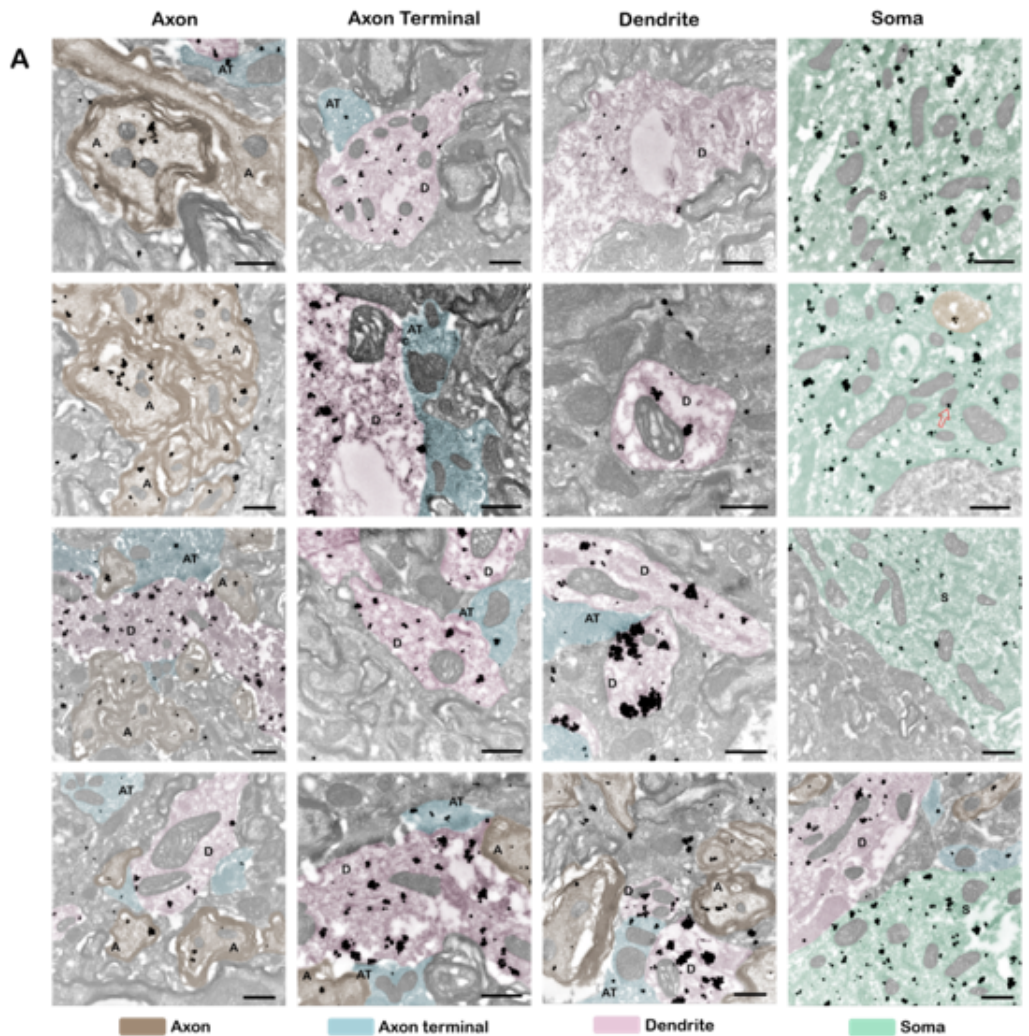


**Figure 13**

Drp1 distribution under TEM A. Drp1 distribution under TEM. The black particulate matter is colloidal gold particles. Brown represents axon, blue represents axon terminal, red represents dendrite, green represents soma. Bar = 500 nm B. Quantity of mitochondria in axon, axon terminal, dendrite and soma. C. Quantity of Drp1 in axon, axon terminal, dendrite and soma. D. Unit area expression of Drp1. According to the test results in Table.1, it can be considered that Drp1 expression was different in axon, axon terminal, dendrite

and cell body. Drp1 expression in dendrites was higher than in axons (adjusted  $P < 0.001$ ), and Drp1 expression in dendrites was higher than in axons terminals (adjusted  $P < 0.001$ ). There was no difference in Drp1 expression between axon and axon terminals, axon and cell bodies, axon terminals and cell bodies, or between dendrites and cell bodies (adjusted  $P > 0.05$ ).

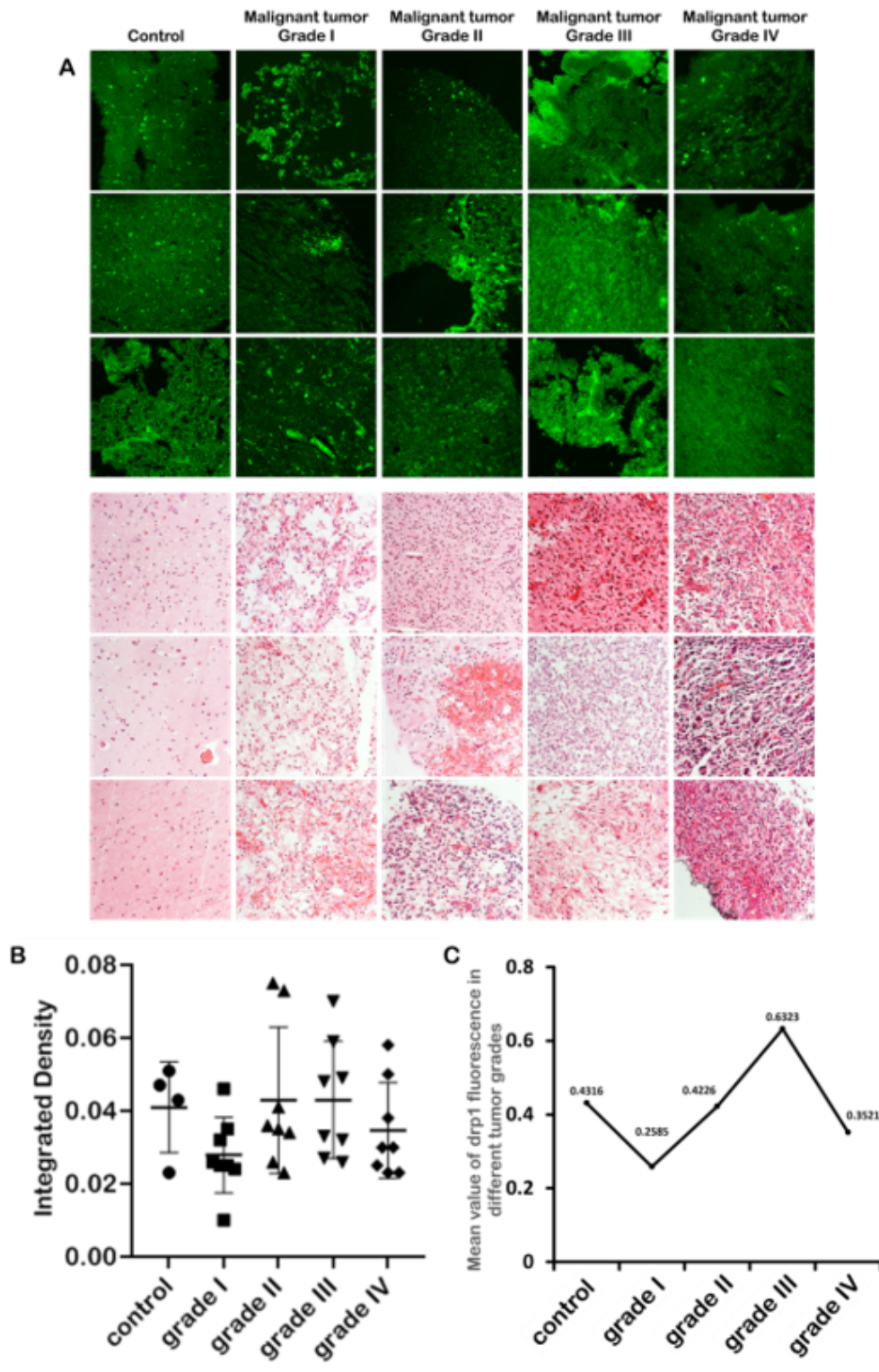
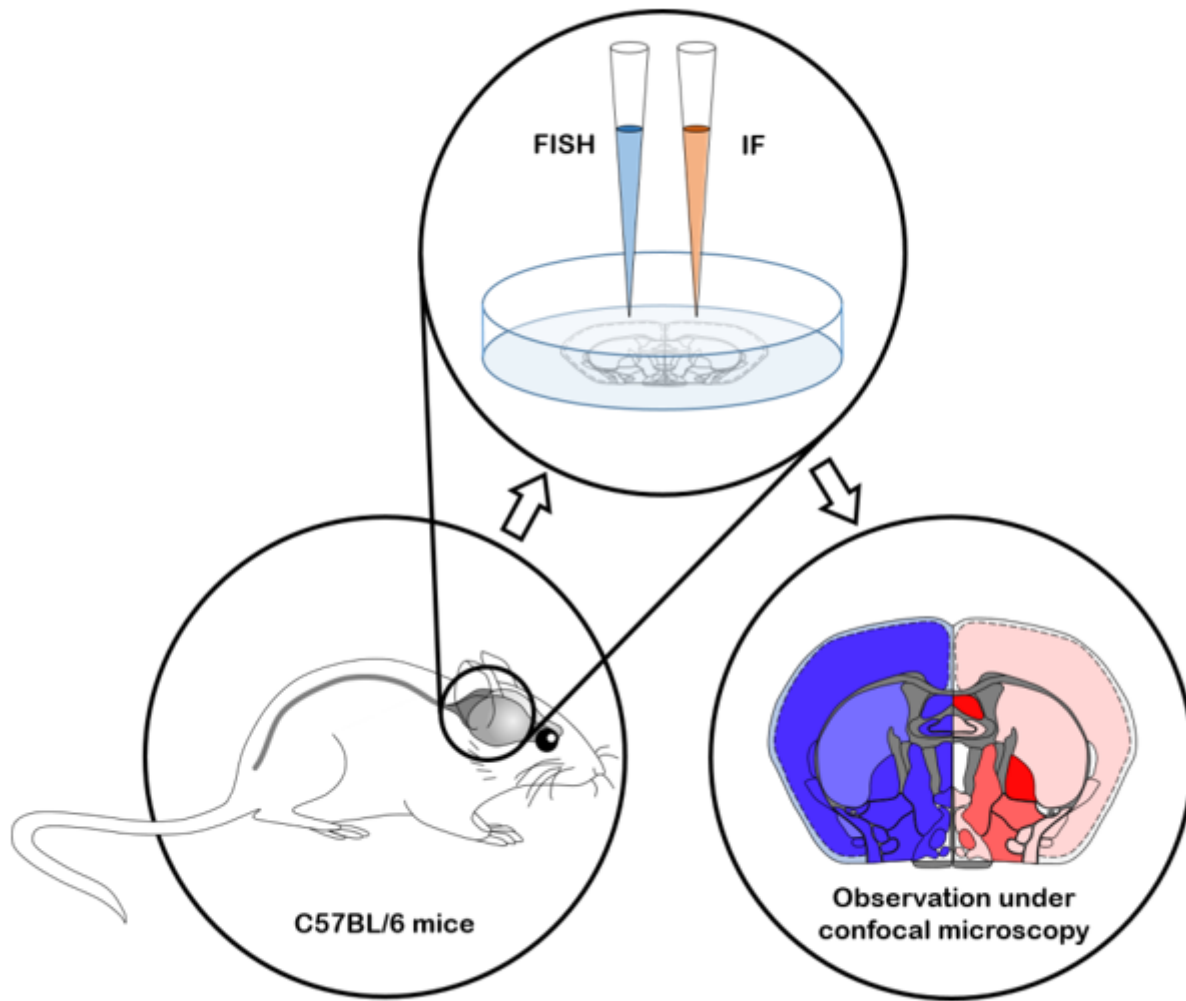


Figure 14

Drp1 expression in human malignant glioma tissue A. Drp1 immunofluorescence staining and same area HE staining in control tissue and human malignant glioma tissue grade I-IV. B, Drp1 expression was different between grade I and grade III, grade III and grade IV ( $P < 0.05$ ) C. Mean value of Drp1 fluorescence intensity in every grade was calculated. From grade I-III, the mean value of Drp1 fluorescence intensity showed an increasing trend. In grade IV, mean value of Drp1 fluorescence intensity significantly reduces.



**Figure 15**

Schematic diagram.1. In order to map the Drp1 protein expression in central nervous system, immunofluorescence staining and FISH were utilized for observation.

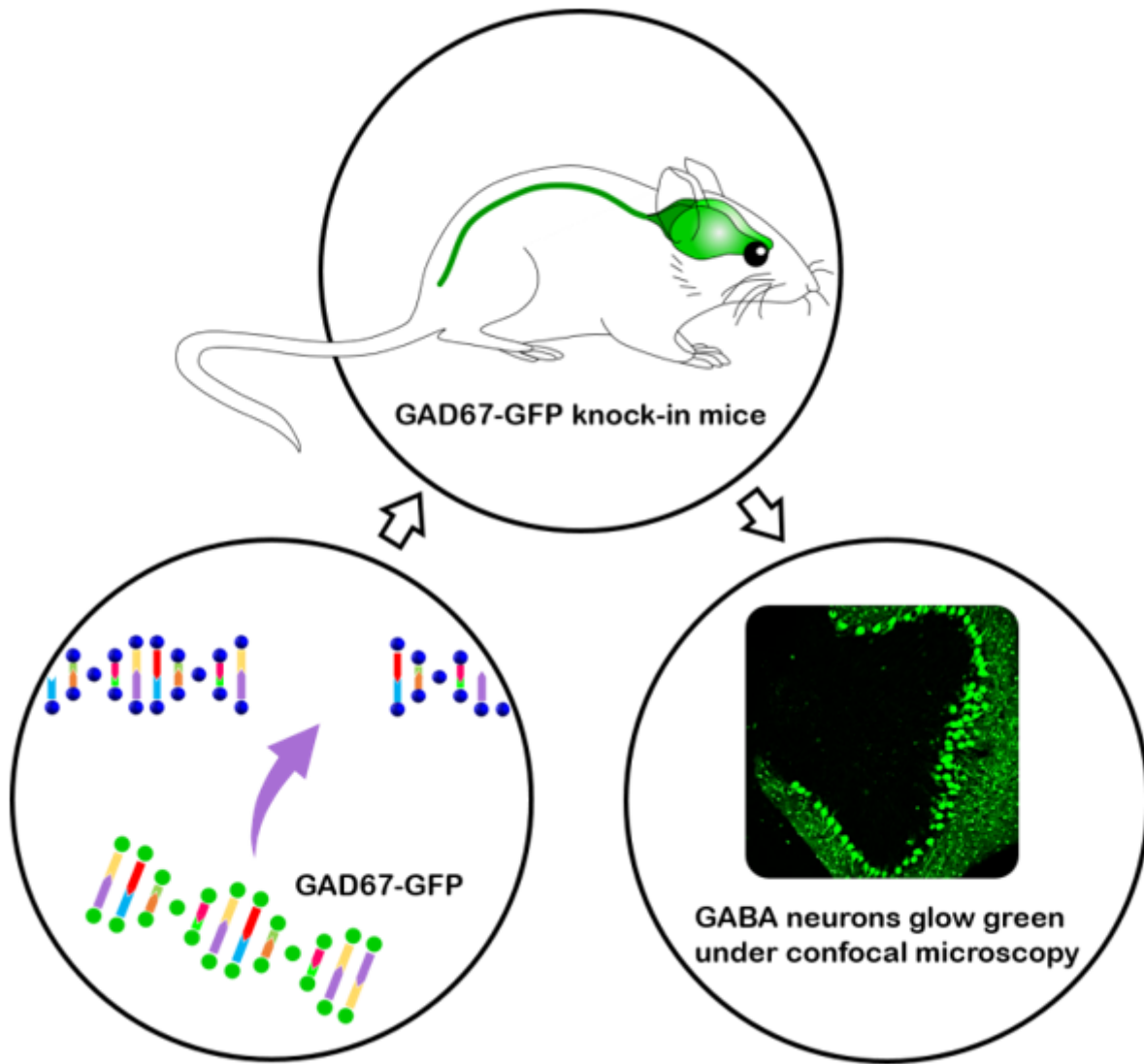


**Figure 16**

Schematic diagram.2 To explore the effect of Drp1 on these diseases, we further clarified the distribution of Drp1 in GABAergic neurons. GAD67-GFP transgenic mice were used to observe the co-labeling of GAD67 and Drp1 in different brain regions.

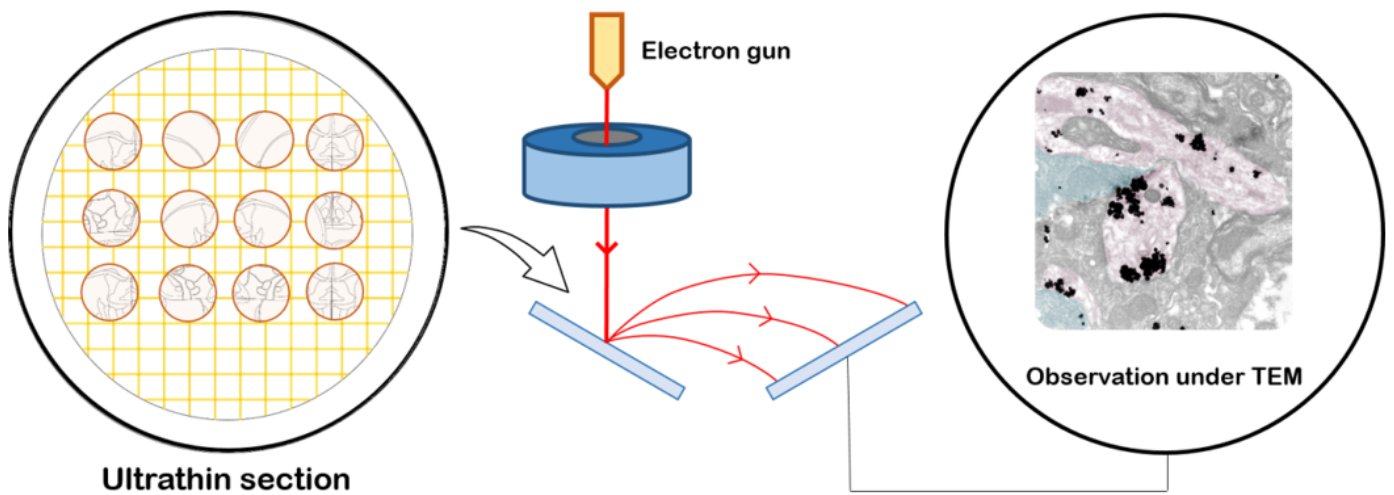


**Figure 17**

Schematic diagram.3 Considering that the fluorescent particles may overlap in vertical space, we utilized electron microscope for further observation. Thus, we next investigated the distribution of mitochondrial Drp1 in PAG brain in the subcellular level through electron microscope.

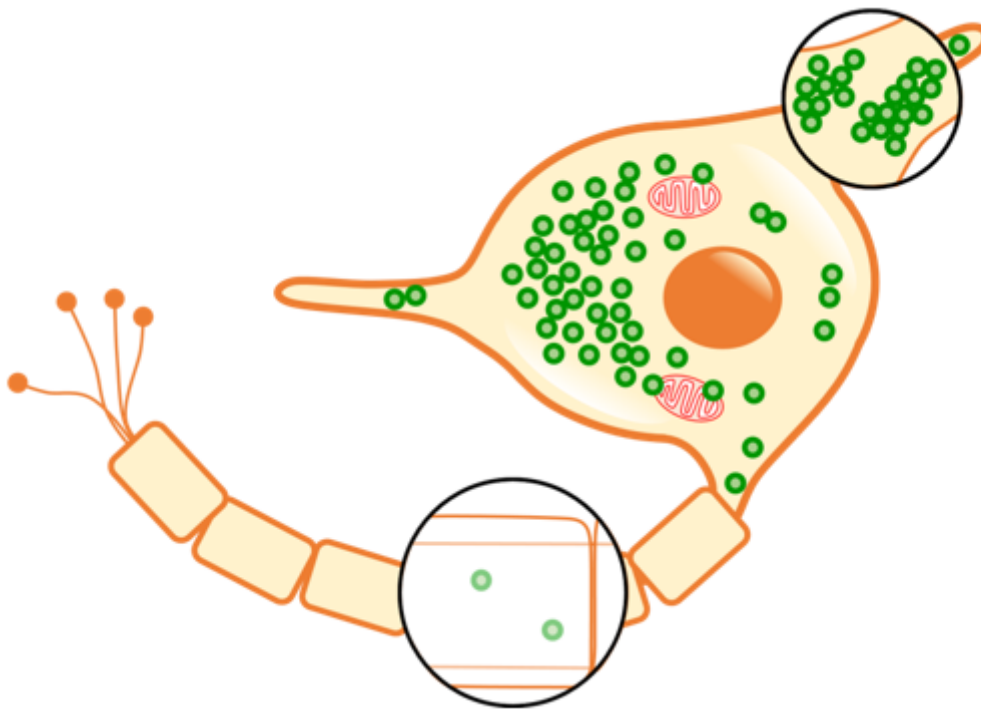


**Figure 18**

Schematic diagram.4 In order to show Drp1 expression in neurons more intuitively, we utilize this schematic diagram for further explanation. Drp1 expression in dendrites was higher than other areas.